INDUCTION SIGNATURES ARE NOT ENOUGH: A MATCHED-COMPUTE STUDY OF LOAD-BEARING STRUCTURE IN IN-CONTEXT LEARNING

Mohammed Sabry
ADAPT Centre, Dublin City University, Ireland
mohammed.sabry@adaptcentre.ie

Anya Belz
ADAPT Centre, Dublin City University, Ireland
anya.belz@dcu.ie

ABSTRACT

Mechanism-targeted synthetic data is increasingly proposed as a way to steer pretraining toward desirable capabilities, but it remains unclear how such interventions should be evaluated. We study this question for in-context learning (ICL) under matched compute (iso-FLOPs) using **Bi-Induct**, a lightweight data rewrite that interleaves short directional copy snippets into a natural pretraining stream: forward-copy (induction), backward-copy (anti-induction, as a directional control), or a balanced mix. Across 0.13B–1B decoder-only models, we evaluate (i) few-shot performance on standard LM benchmarks and function-style ICL probes, (ii) head-level copy telemetry, and (iii) held-out perplexity as a guardrail. Bi-Induct reliably increases induction-head activity, but this does not translate into consistent improvements in few-shot generalization: on standard LM benchmarks, Bi-Induct is largely performance-neutral relative to natural-only training, while on function-style probes the 1B natural-only model performs best. Despite explicit backward-copy cues, anti-induction scores remain near zero across scales, revealing a strong forward/backward asymmetry. Targeted ablations show a sharper distinction: removing the top 2% induction heads per layer harms ICL more than matched random ablations, with the largest relative drop occurring in the natural-only models. This indicates that natural-only training produces more centralized, load-bearing induction circuitry, whereas Bi-Induct tends to create more distributed and redundant induction activity. Our main conclusion is that **eliciting a mechanism is not the same as making it load-bearing**. For data-centric foundation model design, this suggests that synthetic data interventions should be evaluated not only by signature amplification, but by whether they create causally necessary computation while preserving natural-data modeling quality.

1 INTRODUCTION

Transformer language models learn a simple copy pattern early in training: when a token A reappears in context, the model increases the probability of the token that followed the previous A. Prior work identified a two-head motif implementing this behavior and linked it to in-context learning on pattern-matching tasks (Olsson et al., 2022). Despite its simplicity, this motif typically emerges only after many billions of tokens, well after the first training-loss plateau. Theoretical and empirical studies frame the delay as a phase transition (Chen et al., 2024; Edelman et al., 2024). In principle, if one could make induction-like computation become useful earlier in training, this could reduce the compute needed to reach ICL-relevant behaviors and would expose the responsible circuitry sooner for analysis.

A practical way to approach this is to intervene on the *data* rather than the *architecture* or *objective*. In contrast to synthetic-task-only plateau-shortening studies (Kim et al., 2025) and objective-level interventions such as multi-token prediction (Gloeckle et al., 2024), we adopt a data-rewrite perspective that is easy to deploy at scale: inject a small fraction of targeted inputs into the pretraining stream that selectively excite the putative induction mechanism while keeping the architecture and objective fixed. Concretely, we replace a small slice of natural tokens with synthetic copy snippets that cleanly exercise the copier-selector behavior of induction (forward copy) and anti-induction (backward copy). Copy-style cues are the canonical probe for the induction circuit and are widely used to measure it (Olsson et al., 2022; Nanda & Bloom, 2022). While other synthetic families

have been studied (for example n-gram statistics (Edelman et al., 2024), p-hop tasks (Sanford et al., 2024), and intrinsic tasks (Gu et al., 2023)), copy snippets align most directly with the hypothesized mechanism and with distributional properties such as burstiness that correlate with the rise of in-context learning (Chan et al., 2022).

These considerations lead to a single testable question: **under iso-FLOPs, is it more effective for ICL to pretrain purely on natural text, or to allocate a small early-training budget to synthetic directional copy snippets that directly exercise the induction circuit?** Here, "earlier" refers to earlier-peaking induction signatures across layers at a fixed checkpoint under matched compute, not fewer optimization steps to reach a fixed capability.

To answer this, we introduce **Bi-Induct**, a lightweight curriculum that interleaves short duplicate-span snippets with natural text during early training. We evaluate three variants under matched compute: forward induction, backward anti-induction, and a balanced mix where the direction is chosen independently at each injection. We assess each pretraining strategy on three axes: (i) downstream ICL performance on standard few-shot benchmarks and function-style probes; (ii) mechanistic telemetry targeting induction and anti-induction heads; and (iii) held-out perplexity as a quality guardrail. We study these effects across 0.13B, 0.5B, and 1B decoder-only models, using the 0.13B setting as a design lab for span length and mix-ratio selection before scaling the chosen operating point.

Our objective is **not** to present Bi-Induct as a generally superior pretraining recipe. Rather, we use it as a controlled case study for a broader data-centric question: when a synthetic data intervention successfully amplifies a target mechanism, does that mechanism become **causally load-bearing** for downstream behavior, or does it remain a redundant by-product of training? This distinction is especially important for data-centric foundation model design, where synthetic rewrites are attractive because they are easy to deploy, but their practical value depends on whether they improve useful computation rather than merely producing stronger internal signatures.

Contributions:

- **A mechanism-aware evaluation criterion for synthetic data interventions.** We distinguish between **circuit emergence** and **circuit load-bearing**: a targeted mechanism may become visible in telemetry without becoming necessary for task performance.
- **A matched-compute case study of this distinction.** Under iso-FLOPs across 0.13B, 0.5B, and 1B models, we show that Bi-Induct reliably increases induction-head activity but does not reliably improve few-shot ICL, and at 1B the natural-only baseline performs best on function-style probes.
- **Causal evidence via targeted ablation.** Using head-level copy telemetry together with top-2% induction-head ablations, we show that the largest ICL drops occur in the natural-only condition, indicating more centralized, load-bearing induction circuitry there than under Bi-Induct.
- **Directional controls for interpreting copy signals.** By comparing forward induction, backward anti-induction, and a balanced mixture, we find a strong forward/backward asymmetry: even explicit anti-induction training does not materially increase anti-induction scores.
- **Practical lessons for the data-centric design of foundation models (FMs).** Our results suggest that synthetic data interventions should be judged not only by whether they amplify a target signature, but by whether they create behaviorally useful and causally necessary computation without unduly sacrificing natural-data modeling quality.

For a concise glossary of terms and symbols, see Appendix A.

2 Related Work

Induction heads and the mechanics of ICL: The induction-head motif-a two-head circuit that matches a repeated cue and copies its following token-was introduced by Olsson et al. (2022), who provided multiple converging tests linking it to the rise of in-context learning (ICL). Follow-up theory and controlled synthetic-task studies characterize the behavior as a phase transition: on Markov-chain data, models move from uniform predictions to unigram heuristics and then abruptly to bigram induction (Edelman et al., 2024). Provable analyses show that even shallow transformers implement generalized induction via a copier-selector-classifier pipeline, tightening the link between optimization dynamics and the circuit (Chen et al., 2024). At scale, targeted head ablations support causality:

removing a small fraction of high-score induction heads reduces few-shot gains by up to $\sim$32% on abstract pattern tasks and weakens benefits on NLP tasks (Crosbie & Shutova, 2025). Open suites and tools (e.g., Pythia and TransformerLens) have made these effects reproducible across model sizes (Biderman et al., 2023; Nanda & Bloom, 2022).

Anti-induction and copy-suppression circuits: Beyond forward copying, models host heads that suppress copying or implement the backward, "anti-induction" direction. Work on negative heads explains copy suppression as a coherent mechanism that interacts with induction patterns (McDougall et al., 2023). Large-scale empirical reports find a pretrained asymmetry-transformers are stronger at forward induction than backward copy-an imbalance that targeted fine-tuning can reduce while isolating distinct head families (Veitsman et al., 2025). In parallel, Wang et al. (2025) mechanistically link the 'repetition curse' to over-dominant induction heads and propose head-level regularization to restore output diversity.

Curricula that accelerate circuit emergence: A growing line of work seeks to shorten the ICL plateau. Training on diverse ICL tasks in parallel reduces plateau length and eases optimization relative to single-task settings (Kim et al., 2025). Orthogonal to data choice, multi-token prediction modifies the objective to encourage longer-range patterns and shows favorable development of induction-like behaviors together with efficiency gains (Gloeckle et al., 2024). However, these studies concentrate on *forward* induction and are typically evaluated in *synthetic-task-only* training regimes rather than natural-language pretraining, or they rely on objective/architectural changes rather than data-only interventions in end-to-end runs. To our knowledge, they also do not systematically induce or measure *anti*-induction emergence.

Embedding induction heads in downstream systems: Architectural and application work has begun to 'install' n-gram induction heads to stabilize in-context RL and reduce data needs, demonstrating practical leverage of the circuit in agents (Zisman et al., 2025).

Data rewriting: Beyond filtering, recent work rewrites pretraining text to shift style and structure before learning. Rephrasing the Web (WRAP) uses instruction-tuned models to paraphrase web pages into target styles, yielding $\sim 3\times$ faster pretraining on noisy corpora, lower perplexity, and modest zero-shot gains under matched compute budgets (Maini et al., 2024). Nguyen et al. (2025) pursue a related transform-and-retain strategy focused on discarded low-quality documents. Fujii et al. (2025) expand the rewrite paradigm beyond style, reporting boosts on math and code. In parallel, large open datasets such as RefinedWeb show that aggressive deduplication and domain organization improve pretraining without synthetic rewrites, positioning data rewriting as complementary to quality and mixture knobs (Penedo et al., 2023).

Circuit discovery and emergence shaping: Mechanistic interpretability maps internal circuits via activation interventions (Zhang & Nanda, 2024), probing (Gurnee et al., 2023), and increasingly, sparse-autoencoder features (Cunningham et al., 2023). Our focus is earlier in the lifecycle: shaping the data distribution so that desirable circuits appear sooner and more predictably, then verifying the link with head-level telemetry.

Summary: Existing work investigates *circuit discovery/emergence shaping* and, separately, *data rewriting*, but rarely bridges the two-i.e., using mechanistic insight to design pretraining data and evaluating the outcome under matched-compute conditions. We make that link explicit: we target a canonical ICL circuit (forward and backward induction) with the minimal inputs that excite it (directional copy snippets), and compare *pure natural pretraining* to *Bi-Induct*, a small, linearly annealed replacement policy, under iso-FLOPs conditions on the same corpus. We measure effects behaviorally (few-shot ICL benchmarks) and mechanistically (top 2% head concentration by layer), alongside a perplexity guardrail. Unlike prior curricula that emphasize forward copy alone, we study a symmetric forward/backward curriculum side by side to ask whether targeted copy signals are more valuable than additional natural tokens at the same compute.

3 BI-INDUCT

We investigate the effect of *data rewrites* on circuit emergence: we *interleave* synthetic copy snippets into the pretraining stream to explicitly exercise a canonical copy pattern associated with induction. Bi-Induct has two primary variants that differ only in the direction of the copy cue (forward

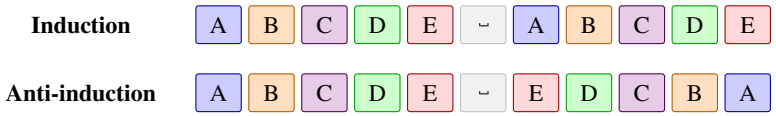

Figure 1: Examples of copy-style snippets injected into the pretraining stream. Each snippet is a span of L random non-special tokens, followed by a separator, then either the same span (induction) or the reversed span (anti-induction). Colors align repeated tokens across the two halves. The illustration uses L=5 for clarity.

vs. backward). A third variant, *balanced*, flips a coin between forward and backward injections to provide a mixed signal.

3.1 Synthetic snippet construction

Let $\mathcal{V}$ be the tokenizer vocabulary and let $\mathrm{BPE}(\cdot)$ be the tokenizer. For a span length L, we first sample a token span

$$S = (s_1, \ldots, s_L), \qquad s_i \sim \mathrm{Uniform}(\{\lfloor 0.05|\mathcal{V}| \rfloor, \ldots, \lfloor 0.95|\mathcal{V}| \rfloor\}),$$

which avoids special/rare IDs. We use a single space as a neutral separator, $\mathrm{SEP} = \mathrm{BPE}(\texttt{" "})$.

Forward/induction (Figure 1, top):

$$\mathrm{Induction}(S) = [S \parallel \mathrm{SEP} \parallel S].$$

Backward/anti-induction (Figure 1, bottom):

$$\mathrm{Anti}(S) = [S \parallel \mathrm{SEP} \parallel \mathrm{reverse}(S)].$$

Balanced (a mix of forward and backward injections): On each injection, flip a fair coin to choose between forward or backward.

Each snippet has length $\ell_{\text{snip}} = 2L + |\mathrm{SEP}|$ (e.g., $2L{+}1$ when SEP is a single space).

3.2 Curriculum schedule and injection rule

We interleave snippets on the fly during streaming pretraining. Let m_0 be the initial mix ratio[1] and T_a an anneal budget (in natural tokens). After t natural tokens have been seen, the instantaneous injection probability is

$$m(t) = \max\{\, m_0 \cdot (1 - t/T_a),\, 0 \,\}.$$

On each natural example, draw $u \sim \mathrm{Uniform}(0, 1)$. If $u < m(t)$, we first yield one synthetic snippet (depending on the current $\texttt{synthetic\_task} \in \{\texttt{induction}, \texttt{anti}, \texttt{balanced}\}$), then yield the natural tokenized sequence. *Else* ($u \geq m(t)$), we emit only the natural tokenized sequence. This implements a light interleave rather than full replacement and keeps the natural distribution dominant.

Expected injection budget ($\bar{m}$): With a linear anneal $m(t) = m_0(1 - t/T_a)$ for $t \in [0, T_a]$ and $m(t){=}0$ afterwards, the *average* injection rate over the anneal is $m_0/2$. Let T_{base} be the natural-token budget of the run. The fraction of injected snippets over the *whole* run is therefore:

$$\bar{m} \;=\; \frac{1}{T_{\text{base}}} \int_0^{T_{\text{base}}} m(t)\, dt \;=\; \begin{cases} m_0/2, & T_a \geq T_{\text{base}}, \\ m_0 \, \dfrac{T_a}{2T_{\text{base}}}, & T_a < T_{\text{base}}. \end{cases}$$

Why this schedule? (i) *Front-loading the signal:* Induction circuits typically emerge after the first loss plateau; concentrating copy cues early helps trigger the phase transition without interfering with

[1] Or mix ratio, for short.

late-stage calibration; (ii) *Stability:* A linear anneal avoids abrupt distribution shifts and exposes a single knob (m_0) for clean sweeps; and (iii) *Compute considerations:* Under standard packing, snippets can share sequences with natural text so the incremental token cost scales with ℓ_{snip} rather than a full segment. We *enforce iso-FLOPs across conditions* (fixed sequence length and optimizer steps), so any potential savings from aggressive packing are intentionally not exploited.[2]

Table 1: Model presets used in experiments. Attention uses head dimension 64; #heads = $\texttt{hidden}/64$ and #KV heads = $\max(1, \lfloor \#\text{heads}/4 \rfloor)$.

Model	Layers	Hidden	MLP (intermediate)	Head dim	#Attn heads	#KV heads
0.13B	12	768	3,072	64	12	3
0.5B	30	1,024	4,096	64	16	4
1B	30	1,536	6,144	64	24	6

4 Experimental Setup

Model: We use a causal decoder-only Transformer with rotary position embeddings (RoPE, θ=10,000), pre-norm residual blocks, and a gated MLP with SiLU activation (SwiGLU). Self-attention uses *grouped key-value attention* (GQA): for head dimension 64, we set number of attention heads = $\texttt{hidden}/64$ and number of KV heads = $\max(1, \lfloor \#\text{heads}/4 \rfloor)$. We train in **bfloat16** with context length 1,024 and *untied* input/output embeddings.[3] Hidden sizes, heads, KV heads, layer counts, and proportional MLP widths are shown in Table 1.

Pretraining data: We pretrain on the deduplicated The Pile dataset (Gao et al., 2020) in streaming/shuffled mode. A stable MD5-based hash assigns a fixed held-out evaluation slice so train/eval partitions remain identical across runs; we set this slice to **0.2%** of the corpus which corresponds to roughly **0.4B** tokens. Tokenization truncates to 1,024 tokens per sequence. Synthetic snippets are interleaved by the Bi-Induct iterator as described in Section 3.

Training recipe: We train all model presets with peak learning rate 1e-3 with linear warmup of 3% of the token budget then cosine decay for the rest. We optimize using AdamW ($\beta_1 = 0.9,\ \beta_2 = 0.999$, weight-decay 0.1), with each update consuming 2^{16} tokens. Following the Chinchilla compute-optimal rule (Hoffmann et al., 2022), we set the total token budget to $T_{base} \approx 20N$ tokens, where N is the number of model non-embedding parameters. We compute the baseline update count as $U = \lceil T_{base}/2^{16} \rceil$ and keep U identical across all *Bi-Induct* curricula at a given scale to enforce iso-FLOPs. We monitor training loss and evaluate perplexity at the final checkpoint on a held-out split of the natural corpus (without synthetic snippets).

Variants: We compare four variants, namely Baseline (no snippets), Induction (forward copy), Anti (backward copy), and Balanced (coin flip per injection).

Metrics and guardrails: We assess Bi-Induct along three complementary axes: (i) *downstream ICL performance* on standard few-shot benchmarks; (ii) *mechanistic telemetry* that targets the intended circuit (induction and anti-induction heads); and (iii) *quality* guardrails. Benchmarks are run few-shot (3-shot by default); we also include function-style tasks from the Todd et al. (2024) suite at 10-shot, evaluated with HITS@1 accuracy to stress simple copy and selection behaviors. For mechanism evidence, we compute per-head copy scores and, at the final checkpoint, report the **top 2%** of heads per layer (and their concentration) for both induction and anti-induction, contrasting Bi-Induct curricula with the baseline. As a guardrail, we report held-out language modeling perplexity (PPL). Table 2 summarizes each metric and its preferred direction; for detailed definitions see Appendix B.

Design lab at 0.13B: We use the **0.13B** model as a design lab to select the operating point for larger-scale runs. Unless noted otherwise, all ablations use a **2.6B** token budget, a **1024** context length, and a **linear anneal over the full budget**.

[2] We fix compute to avoid conflating efficiency optimizations with capability changes; our focus is whether targeted directional copy improves ICL *at the same compute*.

[3] Our architecture largely follows the Mistral-7B design (decoder-only, pre-norm, RoPE, SwiGLU, GQA) (Jiang et al., 2023).

Table 2: Summary of outcome metrics and guardrails. Full definitions in Appendix B.

Family	Metric	What it measures / protocol	Better
Standard LM benchmarks	ICL composite (macro)	Unweighted mean across 3-shot tasks (MMLU, ARC-C, BoolQ, LAMBADA, PIQA; plus others where used). Accuracy or exact match per task; averages over demo seeds.	↑
	Per-task scores	Per-benchmark few-shot evaluation (3-shot by default). Report mean over seeds with the benchmark's standard metric (Acc or EM).	↑
Function probes	ICL composite (macro)	Unweighted mean across ICL tasks probing string manipulation/selection (`capitalize_*`, `next_item`, `word_length`, `alphabetically_*`, `choose_*`). Default 10-shot; metric is HITS@1 accuracy; seeds averaged.	↑
	Per-task scores	Per-probe 10-shot (unless stated) with HITS@1 accuracy; seeds averaged.	↑
Mechanistic telemetry	Head copy score (top 2% per layer)	Per-head induction and anti-induction copy scores at the final checkpoint; report, for each layer, the top 2% heads and their concentration to reveal circuit strength and specialization vs. baseline.	↑
Quality	Perplexity (held-out)	PPL on a fixed 0.2% THE PILE validation slice (stable hash), same tokenizer and context across runs; mean over seeds at iso-FLOPs.	↓

- **Span length (L):** We sweep $L \in \{5, 20, 500\}$ under Bi-Induct and find that L=20 offers the best trade-off between few-shot ICL performance and held-out perplexity. For detailed analysis see Section C.1, Appendix C.
- **Mix ratio (m_0):** With span fixed at L=20, we sweep the initial mix ratio $m_0 \in \{25\%, 50\%, 100\%\}$ (linearly annealed to zero over the full budget). We select **50%** because it yields stronger and more concentrated induction-head activity (top-2% concentration by layer) while maintaining competitive ICL and PPL; see also Section C.2, Appendix C.

Summary and choice for scaling: For the main experiments across **0.13B**, **0.5B**, and **1B**, we adopt L=20 and m_0=50%, which we linearly anneal to 0 over each model's full training token budget (anneal horizon $T_a = T_{\text{base}}$)[4].

5 Natural-Only vs. Directional Copy-Snippet Mix (Iso-FLOPs)

5.1 Downstream ICL Performance

We evaluate two groups of tasks under iso-FLOPs and average over three seeds: (i) *standard LM benchmarks* (14 tasks; e.g., MMLU, BBH, GSM8K, ARC-C, HellaSwag) and (ii) *function-style probes* from the Todd et al. (2024) suite (19 tasks). For the full inventory of *both* groups see Table 5, Appendix B. We report macro-averages per group here and provide per-task scores in Table 8, Appendix D.1.

Standard LM benchmarks: Figure 2a reports 5-shot macro-averages across 14 benchmarks. At each scale, at least one *Bi-Induct* variant matches or very slightly exceeds the natural-only baseline: at 0.13B, *Anti* is closest (22.5 vs. 22.7); at 0.5B, *Induction* leads (23.9 vs. 23.6); at 1B, *Balanced* is on par or marginally higher (24.3 vs. 24.2). Within measurement noise, copy-snippet curricula are *largely performance-neutral* on standard LM benchmarks, but this neutrality is misleading in isolation: function-style probes and targeted ablations reveal important differences in whether induction becomes behaviorally load-bearing.

Function probes (Todd et al., 2024): Figure 2b shows 10-shot macro-averages over 19 probes. At 0.13B and 0.5B, *Bi-Induct* variants are comparable to baseline; at 1B, the natural-only baseline is clearly stronger across the suite.

Robustness checks (1-shot evaluation, label permutation, and shifting the decision rule from HITS@1 to HITS@3) shift absolute scores, but preserve the cross-regime ordering; for details see Appendix D.2.

[4]Annealing over the full budget avoids introducing a second scheduling timescale, reduces re-tuning, and keeps the recipe portable across scales.

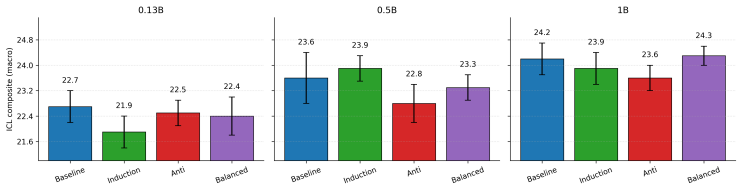

(a)

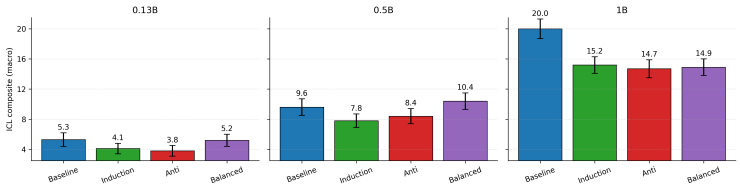

(b)

Figure 2: ICL Composite (macro) across two evaluation families: (a) Standard LM benchmarks; (b) Todd et al. (2024)'s function-probe suite. Each panel groups by model size (0.13B, 0.5B, 1B), bar colors by training regime (Baseline, Induction, Anti, Balanced); error bars show ± 1 s.d. For per-task results see Appendix D.1, Table 8.

5.2 Mechanistic Telemetry

Figure 3 visualizes layerwise copy scores for the top 2% attention heads per layer (with a floor of one head per layer to avoid sampling artifacts). Three clear patterns emerge.

(i) Layerwise localization: At 0.13B and 0.5B, Bi-Induct variants show earlier induction-head emergence than the baseline (by roughly 3 and 2 layers, respectively). At 1B, the trend reverses: the baseline is the first to form clear induction peaks (around layers 10-11) and its early peaks are higher than any Bi-Induct variant. For anti-induction, absolute scores are small at all scales; the largest peak we observe is ≈ 0.04 at 0.5B (Induction curriculum), followed by ≈ 0.02 at 1B (Baseline). In keeping with Veitsman et al. (2025), forward-induction heads dominate in pretrained LMs; in our runs, even the *Anti* curriculum did not materially increase anti-induction copy scores. *Notably, the strongest induction activity is concentrated in mid layers, in keeping with prior observations of where induction heads typically emerge* (Olsson et al., 2022).

(ii) Peak strength: The maximum normalized induction score reaches values close to 1.0 at 0.13B and 0.5B, but stays well below 0.5 at 1B. Thus, even when induction emerges early at 1B (Baseline), its strongest heads are less polarized than at smaller scales.

(iii) Spread: We count heads with a positive copy score among those selected by our per-layer top-2% criterion (Section B.2). Using the best-performing *Bi-Induct* variant at each scale for a like-for-like comparison (Balanced at 0.13B/0.5B; Induction at 1B) we observe: for 0.13B, Baseline 3 vs. Balanced 5; for 0.5B, Baseline 7 vs. Balanced 8; for 1B, Baseline 12 vs. Induction 6. In short, *Bi-Induct* tends to yield earlier and slightly broader induction activity at 0.13B/0.5B, whereas at 1B the natural-only Baseline shows the broader spread.

Link to ICL performance (telemetry vs. causal reliance): The layerwise copy telemetry above is correlational: it localizes where induction-like signatures concentrate, but it does not by itself establish that those heads are *necessary* for ICL. We therefore make a *falsifiable* distinction between *emergence* (telemetry) and *load-bearing* reliance (ablation sensitivity): if stronger/earlier signatures implied necessity, then removing the top induction heads would hurt most precisely in the conditions with the strongest telemetry peaks. Instead, we interpret telemetry jointly with behavioral results and the targeted ablations below.

On standard LM benchmarks (Figure 2a), macro ICL composites are similar across curricula at each scale. In particular, even when Bi-Induct shifts induction signatures toward earlier layers at 0.13B/0.5B, endpoints remain comparable to Baseline; and at 1B, despite the Baseline exhibit-

Table 3: Percent change in the ICL composite on the function-probe suite of Todd et al. (2024) when ablating either the top-2% highest-scoring induction heads per layer(Δ_{induct}) or an equal number of random heads (Δ_{rand}), each measured relative to the model's clean run. Negative values indicate a drop in accuracy; positive values indicate an improvement.

	Baseline		**Induction**		**Anti-induction**		**Balanced**	
Model	Δ_{induct}	Δ_{rand}	Δ_{induct}	Δ_{rand}	Δ_{induct}	Δ_{rand}	Δ_{induct}	Δ_{rand}
0.13B	-22.6%	$+17.0\%$	-4.9%	$+7.3\%$	-5.3%	$+5.3\%$	-19.2%	0.0%
0.5B	-14.6%	-4.2%	-10.3%	$+3.8\%$	-8.3%	-1.2%	-12.5%	0.0%
1B	-19.5%	-4.0%	-14.5%	-2.6%	-12.9%	$+0.7\%$	-8.7%	-4.0%

ing an earlier depth-peak and a broader set of weakly-positive induction heads, Bi-Induct remains broadly competitive on these benchmarks. One plausible explanation is that many of these tasks are knowledge- and calibration-heavy, and larger models can route a substantial fraction of prediction mass through FFN/residual pathways rather than a small set of copy heads (consistent with evidence that FFNs act as key-value memories) (Geva et al., 2021). We treat this as a hypothesis rather than a mechanistic claim.

In contrast, on Todd et al. (2024)'s function-style suite (Figure 2b), the 1B Baseline shows a clear performance advantage, consistent with these probes being more sensitive to explicit copy-head computation. Notably, this advantage does *not* require that the Baseline have more uniformly high-scoring heads: visually (Figure 3), the Baseline is more *concentrated* (dominated by a small subset, including a single prominent head), whereas Bi-Induct variants can exhibit multiple prominent heads yet still fall short on these probes.

Causally, ablating the top-2% induction heads per layer decreases ICL composites more than ablating an equal number of random heads (Table 3). (Occasional small gains from random ablations are consistent with noise/regularization effects.) The relative drop is largest for the natural-only Baseline, while Bi-Induct variants degrade less, consistent with more redundancy or a more distributed implementation of induction-like behavior. A plausible explanation is *front-loaded (in-training) recruitment*: because Bi-Induct injects copy cues early and then anneals them away, it may recruit multiple induction-capable heads that persist as redundant "backup" pathways rather than becoming a single load-bearing bottleneck. Distinguishing early recruitment from late diffusion would require tracking copy telemetry across checkpoints. Detailed per-task comparisons for clean runs vs. induction-head and random-head ablations appear in Table 12, Appendix E.

What might drive the 1B-scale behavior? Two non-exclusive factors may contribute, both consistent with prior literature: (1) *Width-dilution*: the 1B model has the same depth as the 0.5B model but a larger hidden size and more attention heads (24) per layer. As a result, copy behavior may be spread across more heads, reducing the peak score of any single head even if the behavior is present.[5] (2) *Pathway shift*: larger models may increasingly leverage FFN and residual pathways, reducing reliance on localized, high-scoring induction heads (Geva et al., 2021).

Overall, the mechanistic readout suggests that *Bi-Induct consistently accelerates and broadens induction activity at smaller scales*, but *at 1B the natural-only baseline exhibits earlier and broader consolidation of induction*, aligning with its stronger performance on the Todd et al. (2024) suite. In contrast, standard LM few-shot appear largely insensitive to these differences, likely due to the availability of alternative computation pathways.

5.3 Guardrail: Language Modeling Perplexity

Table 4 reports held-out perplexity (mean over three seeds) under iso-FLOPs for each model size. We observe a consistent pattern: the *perplexity gap* between copy-snippet curricula and the baseline *shrinks with scale*, suggesting that larger models can absorb a small synthetic perturbation of the training stream without lasting calibration cost. Qualitatively, this trend is consistent with benign

[5] Prior work finds substantial head redundancy and small subsets of specialized/important heads (Voita et al., 2019; Michel et al., 2019; Olah et al., 2020). In wider models, this redundancy may spread copy behavior across more heads, lowering any single head's score (a speculative 'Width-dilution' effect).

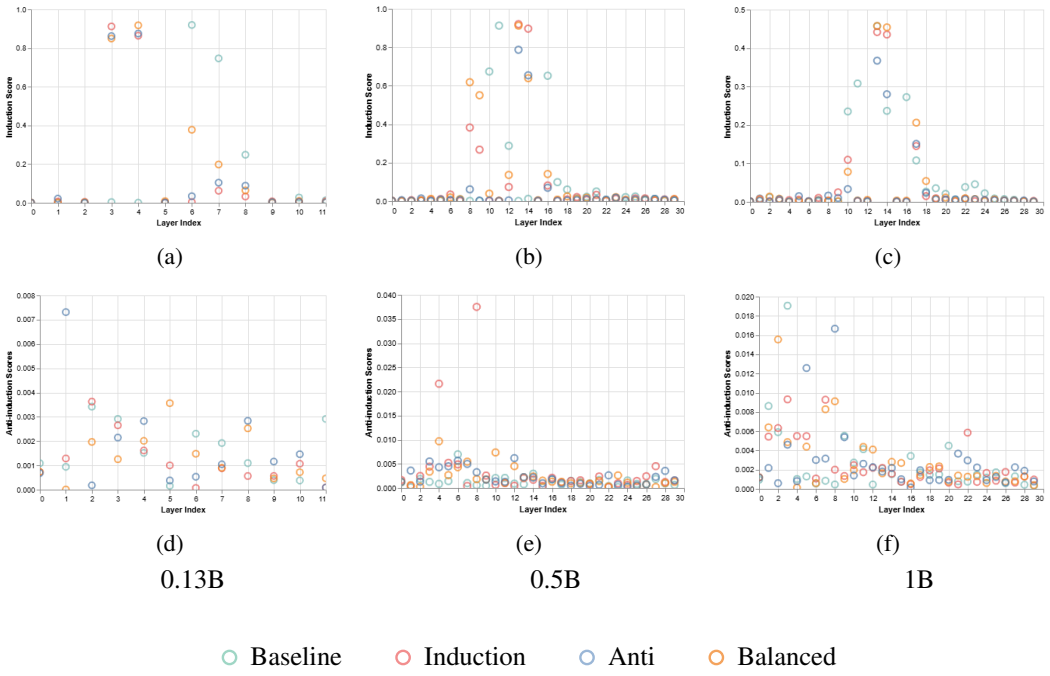

Figure 3: Layer-wise copy-head telemetry. Top row: induction scores; bottom row: anti-induction scores. For each layer we plot the best-scoring head (top 2% by score with a floor of one head per layer), averaged over three seeds, for the 0.13B, 0.5B, and 1B models. Head counts for each model are given in Table 1.

Table 4: Held-out perplexity (PPL ↓) on the fixed THE PILE eval split at iso-FLOPs. Values are averaged over three seeds. For each model size, curricula use a **50%** mix ratio linearly annealed over the full training budget.

Curriculum	**0.13B**	**0.5B**	**1B**
Induction	*25.8*	*17.9*	*14.9*
Anti-induction	*26.2*	*18.2*	*14.9*
Balanced	*26.2*	*18.2*	*14.9*
Baseline	21.8	16.0	14.1

overfitting/double-descent intuitions: larger models can accommodate mild training perturbations while continuing to improve test loss (Nakkiran et al., 2019).

These observations show that a light, annealed Bi-Induct schedule keeps the perplexity penalty bounded and shrinking with scale, but the natural-only baseline remains consistently better on held-out perplexity at every scale.

5.4 IMPLICATIONS FOR DATA-CENTRIC FOUNDATION MODEL DESIGN

Taken together, these results suggest a practical evaluation principle for synthetic data interventions. Under matched compute, it is not sufficient to show that a data rewrite amplifies a target internal signature. A useful intervention should also improve or at least preserve downstream behavior, avoid unnecessary degradation in natural-data modeling quality, and ideally make the targeted computation more causally necessary rather than merely more visible. In our case, Bi-Induct succeeds at signature amplification but not at consistently creating load-bearing ICL circuitry, especially relative to natural-only training at 1B.

6 Conclusion and Future Work

We asked a single matched-compute question: for in-context learning, is it more effective to pretrain purely on natural text, or to allocate a small early-training budget to synthetic directional copy snippets that explicitly exercise the induction circuit? Using Bi-Induct (forward, backward, or balanced injections), we evaluated 0.13B–1B models with three complementary readouts: few-shot ICL performance, head-level copy telemetry, and held-out perplexity.

Bi-Induct reliably amplifies induction signatures, but it does not consistently improve few-shot ICL, and at 1B the natural-only baseline remains more load-bearing. For data-centric foundation model design, the broader lesson is methodological. Synthetic data interventions should not be evaluated only by whether they amplify a desired mechanistic signature. They should also be tested for whether that mechanism becomes **causally necessary** for the downstream behaviors of interest, and whether the intervention preserves natural-language modeling quality. In our study, Bi-Induct is best understood not as a generally superior curriculum, but as a controlled example showing that **signature amplification alone is too weak a success criterion**.

Several directions could extend this study. First, richer synthetic signals that incorporate semantic or linguistic structure may better align with the mechanisms underlying real-world induction behavior than the minimal token-level snippets used here. Second, scaling the analysis to larger models and longer context windows would clarify whether the emergence–vs.–load-bearing distinction persists in regimes where long-context retrieval becomes more critical. Finally, extending this methodology to alternative architectures, such as linear-attention models, may provide insight into whether induction-like behaviors in those systems become structurally necessary for long-context reasoning or remain redundant artifacts of training.

Limitations

Our conclusions are specific to a lightweight copy-based intervention under the conditions studied here. First, the injected snippets are token-level and intentionally minimal; they are not tied to richer linguistic or semantic structure, so our findings should not be read as ruling out more expressive mechanism-aware data rewrites. Second, our study uses final-checkpoint mechanistic analysis and models up to 1B parameters; broader generalization to larger scales remains open. Third, our runs use a context length of 1,024, so we do not claim that the same trade-offs must hold in substantially longer-context settings, where induction-like retrieval may matter more. Finally, because Bi-Induct replaces a fraction of natural data under iso-FLOPs, some of the observed trade-off may reflect natural-text displacement in addition to mechanistic redundancy.

These limitations sharpen, rather than weaken, the main takeaway: mechanism-aware data design should be assessed against a stricter standard than whether it makes a target circuit easier to measure. The key question is whether it makes that circuit matter.

Use of Large Language Models (LLMs)

We used general-purpose large language models as assistive tools for *writing* and *typesetting*. Concretely: (i) LLMs helped draft and polish prose across multiple sections (e.g., Introduction, Related Work, and Conclusion), including line-level rewrites for clarity, grammar, and flow; and (ii) LLMs assisted with LaTeX boilerplate and table scaffolding (e.g., column definitions, `\resizebox`, and `booktabs` structure) but did not determine the content of any table.

LLMs **were not** used to design experiments, analyze data, run code, generate results, or make scientific claims. All technical decisions, datasets, models, and analyses originated from the authors. Every LLM suggestion was reviewed, edited, and verified by the authors; all references and factual statements were cross-checked against primary sources.

References

Aida Amini, Saadia Gabriel, Peter Lin, Rik Koncel-Kedziorski, Yejin Choi, and Hannaneh Hajishirzi. Mathqa: Towards interpretable math word problem solving with operation-based for-

malisms, 2019.

Stella Biderman, Hailey Schoelkopf, Quentin Anthony, Herbie Bradley, Kyle O'Brien, Eric Hallahan, Mohammad Aflah Khan, Shivanshu Purohit, USVSN Sai Prashanth, Edward Raff, Aviya Skowron, Lintang Sutawika, and Oskar van der Wal. Pythia: A suite for analyzing large language models across training and scaling, 2023. URL https://arxiv.org/abs/2304.01373.

Yonatan Bisk, Rowan Zellers, Ronan Le Bras, Jianfeng Gao, and Yejin Choi. Piqa: Reasoning about physical commonsense in natural language. In *Thirty-Fourth AAAI Conference on Artificial Intelligence*, 2020.

Stephanie C. Y. Chan, Adam Santoro, Andrew K. Lampinen, Jane X. Wang, Aaditya Singh, Pierre H. Richemond, Jay McClelland, and Felix Hill. Data distributional properties drive emergent in-context learning in transformers, 2022. URL https://arxiv.org/abs/2205.05055.

Siyu Chen, Heejune Sheen, Tianhao Wang, and Zhuoran Yang. Unveiling induction heads: Provable training dynamics and feature learning in transformers, 2024. URL https://arxiv.org/abs/2409.10559.

Christopher Clark, Kenton Lee, Ming-Wei Chang, Tom Kwiatkowski, Michael Collins, and Kristina Toutanova. BoolQ: Exploring the surprising difficulty of natural yes/no questions. In Jill Burstein, Christy Doran, and Thamar Solorio (eds.), *Proceedings of the 2019 Conference of the North American Chapter of the Association for Computational Linguistics: Human Language Technologies, Volume 1 (Long and Short Papers)*, pp. 2924–2936, Minneapolis, Minnesota, June 2019. Association for Computational Linguistics. doi: 10.18653/v1/N19-1300. URL https://aclanthology.org/N19-1300/.

Peter Clark, Isaac Cowhey, Oren Etzioni, Tushar Khot, Ashish Sabharwal, Carissa Schoenick, and Oyvind Tafjord. Think you have solved question answering? try arc, the ai2 reasoning challenge. *ArXiv*, abs/1803.05457, 2018.

Karl Cobbe, Vineet Kosaraju, Mohammad Bavarian, Jacob Hilton, Reiichiro Nakano, Christopher Hesse, and John Schulman. Training verifiers to solve math word problems, 2021.

Joy Crosbie and Ekaterina Shutova. Induction heads as an essential mechanism for pattern matching in in-context learning. In Luis Chiruzzo, Alan Ritter, and Lu Wang (eds.), *Findings of the Association for Computational Linguistics: NAACL 2025*, pp. 5034–5096, Albuquerque, New Mexico, April 2025. Association for Computational Linguistics. ISBN 979-8-89176-195-7. doi: 10.18653/v1/2025.findings-naacl.283. URL https://aclanthology.org/2025.findings-naacl.283/.

Hoagy Cunningham, Aidan Ewart, Logan Riggs, Robert Huben, and Lee Sharkey. Sparse autoencoders find highly interpretable features in language models, 2023. URL https://arxiv.org/abs/2309.08600.

Ezra Edelman, Nikolaos Tsilivis, Benjamin L. Edelman, eran malach, and Surbhi Goel. The evolution of statistical induction heads: In-context learning markov chains. In *The Thirty-eighth Annual Conference on Neural Information Processing Systems*, 2024. URL https://openreview.net/forum?id=qaRT6QTIqJ.

Kazuki Fujii, Yukito Tajima, Sakae Mizuki, Hinari Shimada, Taihei Shiotani, Koshiro Saito, Masanari Ohi, Masaki Kawamura, Taishi Nakamura, Takumi Okamoto, Shigeki Ishida, Kakeru Hattori, Youmi Ma, Hiroya Takamura, Rio Yokota, and Naoaki Okazaki. Rewriting pre-training data boosts llm performance in math and code, 2025. URL https://arxiv.org/abs/2505.02881.

Leo Gao, Stella Biderman, Sid Black, Laurence Golding, Travis Hoppe, Charles Foster, Jason Phang, Horace He, Anish Thite, Noa Nabeshima, Shawn Presser, and Connor Leahy. The pile: An 800gb dataset of diverse text for language modeling, 2020. URL https://arxiv.org/abs/2101.00027.

Mor Geva, Roei Schuster, Jonathan Berant, and Omer Levy. Transformer feed-forward layers are key-value memories, 2021. URL https://arxiv.org/abs/2012.14913.

Fabian Gloeckle, Badr Youbi Idrissi, Baptiste Rozière, David Lopez-Paz, and Gabriel Synnaeve. Better & faster large language models via multi-token prediction, 2024. URL https://arxiv.org/abs/2404.19737.

Yuxian Gu, Li Dong, Furu Wei, and Minlie Huang. Pre-training to learn in context, 2023. URL https://arxiv.org/abs/2305.09137.

Wes Gurnee, Neel Nanda, Matthew Pauly, Katherine Harvey, Dmitrii Troitskii, and Dimitris Bertsimas. Finding neurons in a haystack: Case studies with sparse probing, 2023. URL https://arxiv.org/abs/2305.01610.

Dan Hendrycks, Collin Burns, Steven Basart, Andy Zou, Mantas Mazeika, Dawn Song, and Jacob Steinhardt. Measuring massive multitask language understanding. *Proceedings of the International Conference on Learning Representations (ICLR)*, 2021.

Jordan Hoffmann, Sebastian Borgeaud, Arthur Mensch, Elena Buchatskaya, Trevor Cai, Eliza Rutherford, Diego de Las Casas, Lisa Anne Hendricks, Johannes Welbl, Aidan Clark, Tom Hennigan, Eric Noland, Katie Millican, George van den Driessche, Bogdan Damoc, Aurelia Guy, Simon Osindero, Karen Simonyan, Erich Elsen, Jack W. Rae, Oriol Vinyals, and Laurent Sifre. Training compute-optimal large language models, 2022. URL https://arxiv.org/abs/2203.15556.

Albert Q. Jiang, Alexandre Sablayrolles, Arthur Mensch, Chris Bamford, Devendra Singh Chaplot, Diego de las Casas, Florian Bressand, Gianna Lengyel, Guillaume Lample, Lucile Saulnier, Lélio Renard Lavaud, Marie-Anne Lachaux, Pierre Stock, Teven Le Scao, Thibaut Lavril, Thomas Wang, Timothée Lacroix, and William El Sayed. Mistral 7b, 2023. URL https://arxiv.org/abs/2310.06825.

Mandar Joshi, Eunsol Choi, Daniel S. Weld, and Luke Zettlemoyer. Triviaqa: A large scale distantly supervised challenge dataset for reading comprehension. In *Proceedings of the 55th Annual Meeting of the Association for Computational Linguistics*, Vancouver, Canada, July 2017. Association for Computational Linguistics.

Jaeyeon Kim, Sehyun Kwon, Joo Young Choi, Jongho Park, Jaewoong Cho, Jason D. Lee, and Ernest K. Ryu. Task diversity shortens the icl plateau, 2025. URL https://arxiv.org/abs/2410.05448.

Pratyush Maini, Skyler Seto, He Bai, David Grangier, Yizhe Zhang, and Navdeep Jaitly. Rephrasing the web: A recipe for compute and data-efficient language modeling, 2024. URL https://arxiv.org/abs/2401.16380.

Callum McDougall, Arthur Conmy, Cody Rushing, Thomas McGrath, and Neel Nanda. Copy suppression: Comprehensively understanding an attention head, 2023. URL https://arxiv.org/abs/2310.04625.

Paul Michel, Omer Levy, and Graham Neubig. Are sixteen heads really better than one?, 2019. URL https://arxiv.org/abs/1905.10650.

Todor Mihaylov, Peter Clark, Tushar Khot, and Ashish Sabharwal. Can a suit of armor conduct electricity? a new dataset for open book question answering. In *EMNLP*, 2018.

Sewon Min, Xinxi Lyu, Ari Holtzman, Mikel Artetxe, Mike Lewis, Hannaneh Hajishirzi, and Luke Zettlemoyer. Rethinking the role of demonstrations: What makes in-context learning work?, 2022. URL https://arxiv.org/abs/2202.12837.

Preetum Nakkiran, Gal Kaplun, Yamini Bansal, Tristan Yang, Boaz Barak, and Ilya Sutskever. Deep double descent: Where bigger models and more data hurt, 2019. URL https://arxiv.org/abs/1912.02292.

Neel Nanda and Joseph Bloom. Transformerlens. https://github.com/TransformerLensOrg/TransformerLens, 2022.

Thao Nguyen, Yang Li, Olga Golovneva, Luke Zettlemoyer, Sewoong Oh, Ludwig Schmidt, and Xian Li. Recycling the web: A method to enhance pre-training data quality and quantity for language models, 2025. URL https://arxiv.org/abs/2506.04689.

Chris Olah, Nick Cammarata, Ludwig Schubert, Gabriel Goh, Michael Petrov, and Shan Carter. Zoom in: An introduction to circuits. *Distill*, 5(3):e00024.001, March 2020. doi: 10.23915/distill.00024.001. URL https://distill.pub/2020/circuits/zoom-in/.

Catherine Olsson, Nelson Elhage, Neel Nanda, Nicholas Joseph, Nova DasSarma, Tom Henighan, Ben Mann, Amanda Askell, Yuntao Bai, Anna Chen, Tom Conerly, Dawn Drain, Deep Ganguli, Zac Hatfield-Dodds, Danny Hernandez, Scott Johnston, Andy Jones, Jackson Kernion, Liane Lovitt, Kamal Ndousse, Dario Amodei, Tom Brown, Jack Clark, Jared Kaplan, Sam McCandlish, and Chris Olah. In-context learning and induction heads. *Transformer Circuits Thread*, 2022. https://transformer-circuits.pub/2022/in-context-learning-and-induction-heads/index.html.

Denis Paperno, Germán Kruszewski, Angeliki Lazaridou, Quan Ngoc Pham, Raffaella Bernardi, Sandro Pezzelle, Marco Baroni, Gemma Boleda, and Raquel Fernández. The lambada dataset, Aug 2016.

Guilherme Penedo, Quentin Malartic, Daniel Hesslow, Ruxandra Cojocaru, Alessandro Cappelli, Hamza Alobeidli, Baptiste Pannier, Ebtesam Almazrouei, and Julien Launay. The refinedweb dataset for falcon llm: Outperforming curated corpora with web data, and web data only, 2023. URL https://arxiv.org/abs/2306.01116.

David Rein, Betty Li Hou, Asa Cooper Stickland, Jackson Petty, Richard Yuanzhe Pang, Julien Dirani, Julian Michael, and Samuel R. Bowman. Gpqa: A graduate-level google-proof q&a benchmark, 2023.

Keisuke Sakaguchi, Ronan Le Bras, Chandra Bhagavatula, and Yejin Choi. Winogrande: An adversarial winograd schema challenge at scale. *arXiv preprint arXiv:1907.10641*, 2019.

Clayton Sanford, Daniel Hsu, and Matus Telgarsky. Transformers, parallel computation, and logarithmic depth, 2024. URL https://arxiv.org/abs/2402.09268.

Mirac Suzgun, Nathan Scales, Nathanael Schärli, Sebastian Gehrmann, Yi Tay, Hyung Won Chung, Aakanksha Chowdhery, Quoc V Le, Ed H Chi, Denny Zhou, , and Jason Wei. Challenging big-bench tasks and whether chain-of-thought can solve them. *arXiv preprint arXiv:2210.09261*, 2022.

Alon Talmor, Jonathan Herzig, Nicholas Lourie, and Jonathan Berant. CommonsenseQA: A question answering challenge targeting commonsense knowledge. In *Proceedings of the 2019 Conference of the North American Chapter of the Association for Computational Linguistics: Human Language Technologies, Volume 1 (Long and Short Papers)*, pp. 4149–4158, Minneapolis, Minnesota, June 2019. Association for Computational Linguistics. doi: 10.18653/v1/N19-1421. URL https://aclanthology.org/N19-1421.

Eric Todd, Millicent L. Li, Arnab Sen Sharma, Aaron Mueller, Byron C. Wallace, and David Bau. Function vectors in large language models, 2024. URL https://arxiv.org/abs/2310.15213.

Yana Veitsman, Mayank Jobanputra, Yash Sarrof, Aleksandra Bakalova, Vera Demberg, Ellie Pavlick, and Michael Hahn. Born a transformer – always a transformer?, 2025. URL https://arxiv.org/abs/2505.21785.

Elena Voita, David Talbot, Fedor Moiseev, Rico Sennrich, and Ivan Titov. Analyzing multi-head self-attention: Specialized heads do the heavy lifting, the rest can be pruned. In Anna Korhonen, David Traum, and Lluís Màrquez (eds.), *Proceedings of the 57th Annual Meeting of the Association for Computational Linguistics*, pp. 5797–5808, Florence, Italy, July 2019. Association for Computational Linguistics. doi: 10.18653/v1/P19-1580. URL https://aclanthology.org/P19-1580/.

Shuxun Wang, Qingyu Yin, Chak Tou Leong, Qiang Zhang, and Linyi Yang. Induction head toxicity mechanistically explains repetition curse in large language models, 2025. URL https://arxiv.org/abs/2505.13514.

Jerry Wei, Jason Wei, Yi Tay, Dustin Tran, Albert Webson, Yifeng Lu, Xinyun Chen, Hanxiao Liu, Da Huang, Denny Zhou, and Tengyu Ma. Larger language models do in-context learning differently, 2023. URL https://arxiv.org/abs/2303.03846.

Kayo Yin and Jacob Steinhardt. Which attention heads matter for in-context learning?, 2025. URL https://arxiv.org/abs/2502.14010.

Rowan Zellers, Ari Holtzman, Yonatan Bisk, Ali Farhadi, and Yejin Choi. Hellaswag: Can a machine really finish your sentence? In *Proceedings of the 57th Annual Meeting of the Association for Computational Linguistics*, 2019.

Fred Zhang and Neel Nanda. Towards best practices of activation patching in language models: Metrics and methods, 2024. URL https://arxiv.org/abs/2309.16042.

Tony Z. Zhao, Eric Wallace, Shi Feng, Dan Klein, and Sameer Singh. Calibrate before use: Improving few-shot performance of language models, 2021. URL https://arxiv.org/abs/2102.09690.

Ilya Zisman, Alexander Nikulin, Viacheslav Sinii, Denis Tarasov, Nikita Lyubaykin, Andrei Polubarov, Igor Kiselev, and Vladislav Kurenkov. N-gram induction heads for in-context rl: Improving stability and reducing data needs, 2025. URL https://arxiv.org/abs/2411.01958.

A Glossary and Terminology

This section defines the terms and metrics used throughout the paper. We group entries by theme for quick reference.

Copy-style circuits and interpretability

Mechanistic interpretability The study of internal circuits and features that give rise to behavior in neural networks. Typical tools include ablations/masking, activation patching, causal tracing, and sparse autoencoders.

Interpretability challenges Practical difficulties include superposition (features sharing parameters), circuit non-uniqueness (multiple decompositions fit the data), intervention fragility (ablations can misattribute causality), scale transfer (circuits shift across sizes), and dataset confounds (spurious correlations masquerading as mechanisms).

Induction head / induction circuit A two-head attention motif that implements forward copy: when a cue token reappears in the context, attention retrieves what followed the *previous* occurrence and predicts it again. Empirically linked to few-shot pattern matching.

Anti-induction The mirror of induction: backward copy. Given a repeated cue, the model predicts the *preceding* token from an earlier occurrence (useful for reversal-style tasks and some code transforms).

Copy-suppression (negative) heads Attention heads whose contribution reduces copying (e.g., down-weights repeated spans), often interacting with induction heads to prevent degenerate repetition.

Curriculum and data-rewrite terms

Data rewrite Deliberate modification of a small fraction of pretraining tokens to teach a target algorithm (here, copy patterns) without changing the model architecture.

Bi-Induct Our symmetric copy-style curriculum that injects synthetic snippets during pretraining in one of two directions: `induction` (forward copy) or `anti` (backward copy). Injection probability linearly anneals to zero.

Span length (L) Number of random tokens in the snippet's base span before duplication or reversal (e.g., $L \in \{5, 20, 100\}$).

(Initial) Mix ratio Initial probability of injecting a synthetic snippet before annealing (e.g., 25%).

Anneal tokens The number of natural tokens over which the injection probability decays linearly to zero (e.g., the full 2.5B-token budget).

"Balanced" variant A coin-flip per injection between forward and backward copy. Used as an additional control in some ablations.

COMPUTE AND EFFICIENCY

Chinchilla (compute-optimal) budget The token-parameter trade-off that minimizes validation loss at fixed compute for dense decoder-only LMs. Rule of thumb: a tokens-to-parameters ratio of $\approx$ 20:1, i.e., $T \approx 20N$ (tokens T, parameters N).

EVALUATION ENDPOINTS

ICL benchmarks (few-shot endpoints) Standard few-shot ($k \geq 1$) tasks evaluated at the *final* checkpoint (e.g., 3-shot MMLU, ARC-C, BoolQ, LAMBADA, PIQA). We aggregate with a macro-average as the **ICL composite**. These are the *main* outcome metrics. *Regarding the standard deviation (s.d.) of the ICL composite:* In Tables 6 and 7, we compute the s.d. of the per-seed composite across seeds, which is the appropriate uncertainty. Elsewhere, for brevity, we approximate the composite's uncertainty by averaging per-task s.d.s computed across seeds; this is a readable proxy but not a pooled s.d. and it ignores cross-task covariance.

Cross-entropy and perplexity Language-model loss on a held-out split of the pretraining corpus. Perplexity $\mathrm{PPL} = \exp(\mathrm{CE})$. Used as a quality and calibration guardrail.

B METRICS AND GUARDRAILS: DETAILED DEFINITIONS

B.1 BENCHMARKS AND PROTOCOLS

Aggregation: We report a *macro* ICL composite (unweighted mean across selected tasks) and per-task scores. All figures and tables show mean over seeds. Full list of benchmarks used is in table 5

Prompting controls: For few-shot tasks, we fix a template and average across multiple demonstration seeds. For robustness, we randomize demonstration order and, in §D.2, evaluate sensitivity to number of shots and a label-permutation stress test.

B.2 MECHANISTIC TELEMETRY

Targeted circuits: We measure two equality-based copy circuits-*induction* and *anti-induction*-highlighted in prior work(e.g., (Olsson et al., 2022; Veitsman et al., 2025)).[6]. In a left-to-right causal decoder, *attention flows from the later span back to the earlier span*. Consider a repeated sequence $x = s_0\, s_1\, \ldots\, s_{L-1}\, \langle \mathrm{sep} \rangle\, s'_0\, s'_1\, \ldots\, s'_{L-1}$ with $s'_i = s_i$:

- *Induction (forward copy).* At position s'_i in the second span, the head locates the earlier repeat and retrieves payload that helps predict the *next* token s'_{i+1}. We operationalize this with a *next-token* alignment (defined below).
- *Anti-induction (backward copy).* At position s'_i, the head again locates the earlier repeat but retrieves payload that helps predict the token immediately to the *left*, s'_{i-1}. We operationalize this with a *same-token* alignment (defined below).

Probe sequences: We evaluate on $50{,}000$ fresh copy probes disjoint from training, each built as $x = s\, \langle \mathrm{sep} \rangle\, s$ with a uniformly sampled token span s of length $L{=}500$[7].

[6] See also (Wang et al., 2025; Yin & Steinhardt, 2025).

[7] We evaluate with a span length of $L = 500$ (rather than $L = 20$) to reduce potential confounds from the *Bi-Induct* pretraining curriculum, which used $L = 20$.

Per-head scores (how we compute them): Let $A^{(\ell,h)} \in \mathbb{R}^{T\times T}$ be the attention map (rows = target positions, columns = source positions) for layer ℓ, head h on x. Index t_i as the row of s'_i (second span) and m_i as the column of s_i (first span).

Induction (next-token) score: Using $\mathcal{D}_{\text{next}} = \{(t_i, m_{i+1})\}_{i=0}^{L-2}$ (later s'_i to earlier s_{i+1}),

$$\text{Score}_I(\ell,h) \;=\; \mathbb{E}_x\left[\frac{1}{L-1}\sum_{(t_i,m_{i+1})\in\mathcal{D}_{\text{next}}} A^{(\ell,h)}_{t_i,m_{i+1}}\right].$$

Anti-induction (same-token) score: Using the same-token diagonal $\mathcal{D}_{\text{same}} = \{(t_i, m_i)\}_{i=0}^{L-1}$ (later s'_i to earlier s_i),

$$\text{Score}_A(\ell,h) \;=\; \mathbb{E}_x\left[\frac{1}{L}\sum_{(t_i,m_i)\in\mathcal{D}_{\text{same}}} A^{(\ell,h)}_{t_i,m_i}\right].$$

Higher is better for both Score_I and Score_A (stronger, more localized copy behavior).

Top 2% concentration by layer: Let H_ℓ be the heads in layer ℓ and $k_\ell = \max\{1, \lceil 0.02\,|H_\ell|\rceil\}$. For $Score \in \{Score_I, Score_A\}$, let $\text{Top}_\ell(S)$ be the k_ℓ heads with largest $S(\ell,h)$. We report the mass share

$$\text{MassShare}_\ell^{(Score)} = \frac{\sum_{h\in\text{Top}_\ell(Score)} Score(\ell,h)}{\sum_{h\in H_\ell} Score(\ell,h)},$$

and the layer mean $\overline{S}core_\ell = \frac{1}{|H_\ell|}\sum_{h\in H_\ell} Score(\ell,h)$. Larger values indicate stronger specialization (copy mass concentrated in a few heads).

B.3 Language modeling quality

Perplexity: We compute cross-entropy and PPL on a fixed 0.2% The Pile validation slice (stable hash partition), at iso-FLOPs and identical tokenization settings across runs.

C Ablation Study

C.1 Span length

We begin by testing how the snippet span L affects outcomes. At **0.13B**, with a fixed initial mix of 25% linearly annealed over the full token budget, we sweep $L \in \{5, 20, 500\}$ and report two endpoints of practical interest-(i) a 5-shot ICL composite over five standard LM benchmarks and (ii) held-out LM perplexity (PPL). We defer the function-probe suite of Todd et al. (2024) to the cross-scale experiments, where relative differences are more interpretable and the added compute is justified; the span-length results for this subsection are summarized in Table 6.

Across curricula, L=20 is a stable operating point that balances ICL and calibration: for *Induction*, 31.9 ICL / 23.9 PPL (vs. 30.7/23.8 at L=5 and 31.8/24.0 at L=500); for *Anti*, 32.1/24.0 (vs. 31.6/23.8 at L=5 , 31.7/24.5 at L=500) respectively; for *Balanced*, 31.2/24.0 (vs.31.4/23.8 at L=5, 32.0/24.0 at L=500). Very short spans (L=5) underperform on the ICL composite, while very long spans (L=500) offer no consistent ICL gain and tend to slightly worsen PPL. Hence we adopt L=20 for the remaining experiments. Beyond the ICL / PPL balance, shorter spans are operationally attractive: they minimize snippet length $2L+|\text{SEP}|$, which reduces potential overhead and makes it easier to *pack* snippets alongside natural sequences to exploit variable-length kernels-yielding compute savings when such packing is enabled.[8]

C.2 Mix Ratio

We fixed the anneal to the *full* training budget (2.6B token, following the Chinchilla parameter-token rule of thumb (Hoffmann et al., 2022)), held the span length at L=20, and swept the initial mix ratio over {25%, 50%, 100% }. Table 7 reports full per-task results.

[8] All reported results are at iso-FLOPs; we do *not* take packing credits in our comparisons. Packing is a deployment optimization, not part of the evaluation protocol.

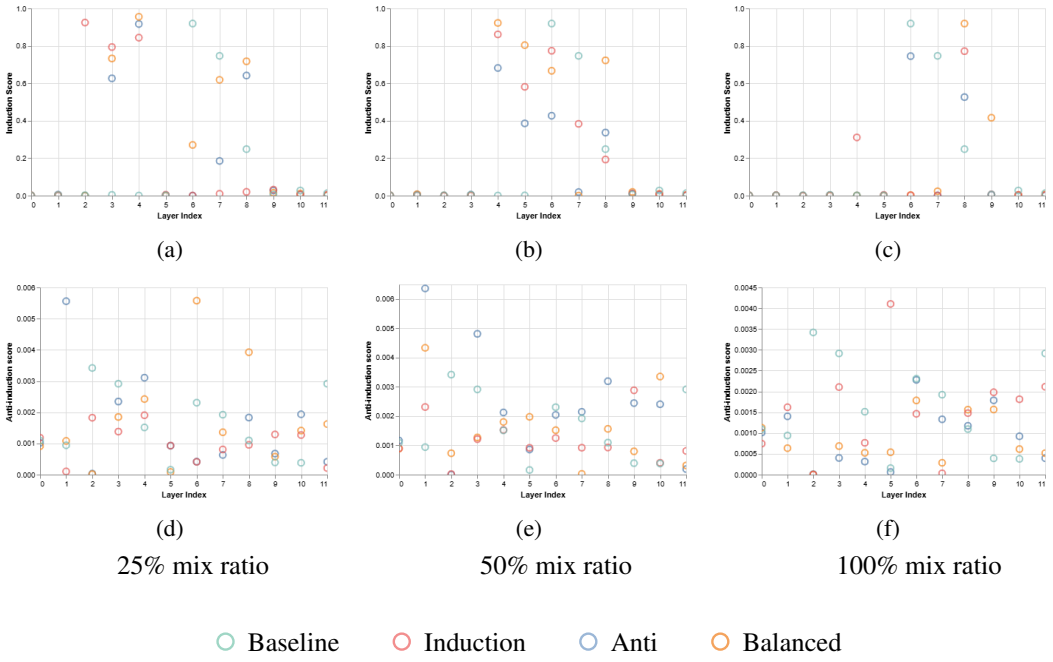

Figure 4: Layer-wise copy-head telemetry. Top row: induction scores; bottom row: anti-induction scores. For each layer we plot the best-scoring head (top 2% by score with a floor of one head per layer), averaged over six seeds, for the 0.13B model with initial mix ratios: 25%, 50%, and 100% . Head counts for each model are given in Table 1.

Mechanistic readout: Figure 4 summarizes layerwise copy-head activity across mix ratios. We quantify head quality in two complementary ways: (i) *spread*, the number of heads per model whose induction score is non-zero (and, for comparability, the count above a fixed "specialization" threshold > 0.5); and (ii) *peak sharpness*, the maximum head score in each condition. We also note *concentration* in depth (whether peaks cluster in the canonical mid-layers).

Does synthetic injection improve induction-head quality vs. baseline? By counts above the 0.5 threshold, yes up to moderate mixes. The baseline shows 2 specialized heads. With **Induction** snippets we observe $\{3, 3, 1\}$ specialized heads at $\{25\%, 50\%, 100\%\}$ mixes, **Balanced** yields $\{4, 4, 1\}$, and **Anti** yields $\{3, 1, 2\}$. By peak sharpness, **Balanced-25%** attains the highest induction head, with Induction and Anti close behind; at $\geq 50\%$ mixes, Balanced and Baseline retain similar peaks while Induction then Anti trail.

Does the curriculum create anti-induction heads? No. Even under Anti mixes, anti-induction scores remain far below the specialization threshold; the best peaks are ≈ 0.01 (at 50% Anti and in Baseline), indicating no robust anti-induction circuit emerges.

How does mix ratio affect spread and depth concentration (induction)? For **Induction**, spread rises from 25% to 50% (3→5 heads) then contracts at 100% (2). For **Balanced**, spread is largest at 25% (5), then declines (4 at 50%, 2 at 100%). For **Anti**, induction heads peak at 25-50% (4 each) and drop to 2 at 100%. Depthwise, specialized heads shift deeper as mix increases: clusters are earlier at 25% (layers ∼2-4), mid-depth at 50% (layers ∼4-6), and later at 100% (around layer ∼8).

Takeaways: Baseline naturally forms a few strong induction heads. Adding snippets increases the *number* of specialized induction heads up to moderate mixes ($\leq 50\%$); higher mixes reduce spread and push peaks deeper. None of the curricula-especially Anti-produces meaningful anti-induction heads.

D In-Context Learning Capability

D.1 In-Context Learning Performance

In Table 8 (summarized in Figure 2a and Figure 2b; see §5.1), we report *per-task* few-shot ICL performance across scales for two families: (i) 14 standard LM benchmarks/tasks and (ii) 19 function-style probes from the Todd et al. (2024) suite. For the standard LM benchmarks we use **3-shot** evaluation; for the Todd et al. (2024) suite we use **10-shot** evaluation. (Table 5 lists all tasks and provides a brief description of each.) Unless otherwise noted, metrics are accuracy (ACC) or exact match (EM) as standard, and all results are averaged over three seeds.

Because any > 0 shot setting exercises in-context learning, we also study **1-shot** sensitivity for the same tasks/benchmarks in Appendix D.2.

D.2 In-Context Learning Robustness

D.2.1 Sensitivity to Number of Shots

We assess how the ICL results in §5.1 (with details in Appendix D.1) vary with the number of in-context demonstrations. Concretely, we change the evaluation from the main-text setting (3-shot for standard LM benchmarks and 10-shot for function-probe tasks) to a unified 1-shot setting for both families. Summaries appear in Figure 5a (standard LM) and Figure 5b (function probes); per-task scores are in Table 9.

For the standard LM benchmarks, moving to 1-shot produces negligible changes across all model sizes (0.13B, 0.5B, 1B). In contrast, the function-style probes degrade notably at 0.5B and 1B when reduced to 1-shot, while the 0.13B model shows only a small drop. This scale-dependent sensitivity aligns with prior observations that larger models more reliably use the demonstration label→token mapping (and thus benefit from more shots), whereas smaller models often gain primarily from format/structure and topical priming (Wei et al., 2023; Min et al., 2022; Zhao et al., 2021). Consistently, our label-permutation stress test shows minimal impact at 0.13B but clear degradation at 0.5B/1B, indicating that bigger models lean more on the (now corrupted) mapping signal.

Across shot conditions, the Baseline vs. Bi-Induct ordering remains stable: reducing shots changes the absolute level but not the ranking among curricula.

D.2.2 Function-Probe Task Stress Tests

Because stress tests were explicitly considered during the development of the Todd et al. (2024) function-probe suite, we evaluate two that directly target ICL robustness: (i) *label permutation* within the in-context demonstration shots, and (ii) *decision-rule sensitivity*, contrasting the commonly reported HITS@3 with our primary metric, HITS@1. These tests probe robustness to spurious label-token mappings and to the choice of evaluation rule, respectively.

Label-Permutation Stress Test: We stress-test in-context usage on the Todd et al. (2024) probes by randomly permuting the targets within the 10 demonstration shots (inputs unchanged) and evaluating on the true task distribution. If a model relies on the demonstrations, accuracy should drop; if it leans on parametric priors, it should be less affected. As shown in Figure 6 and Table 10, the relative ordering between Baseline and Bi-Induct variants is largely preserved. At **0.13B**, permutation produces no degradation for either, suggesting heavier reliance on parametric knowledge. At **0.5B** and **1B**, all curricula degrade, indicating increased sensitivity to the in-context mapping. Overall, Bi-Induct mirrors Baseline at each scale: robust at 0.13B and increasingly demonstration-sensitive as scale grows.

Why permutation hurts 0.5B-1B but not 0.13B? At 0.13B, the robustness to label permutation suggests it benefits from demonstrations via format/topical priming and answer-frequency priors, but does not reliably exploit the label→token mapping. In contrast, 0.5B-1B models more strongly use the in-context mapping; permuting labels therefore contradicts a cue they have learned to trust, producing clear drops. This is consistent with reports that (i) labels in demos can be non-essential for smaller/less capable settings-format and priors often dominate (Min et al., 2022; Zhao et al.,

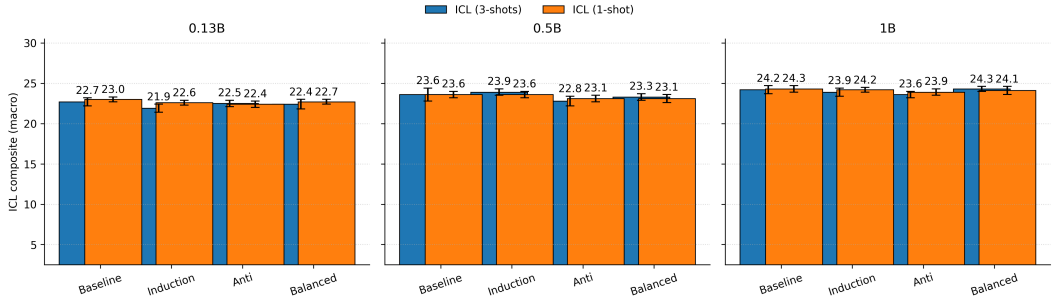

(a)

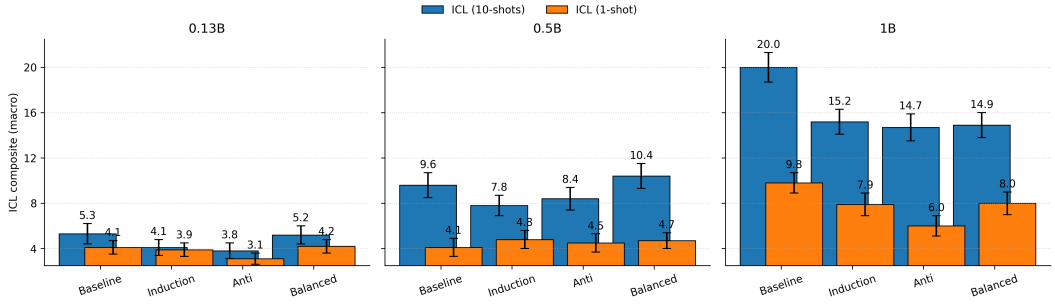

(b)

Figure 5: Sensitivity of ICL composite (macro) to the number of shots across two evaluation families: (a) standard LM benchmarks (3-shot vs. 1-shot); (b) Function-probe suite of Todd et al. (2024) (10-shot vs. 1-shot). Each panel groups models by size (0.13B, 0.5B, 1B), colors the bars by regime (Baseline, Induction, Anti, Balanced), and shows ± 1 s.d. error bars.

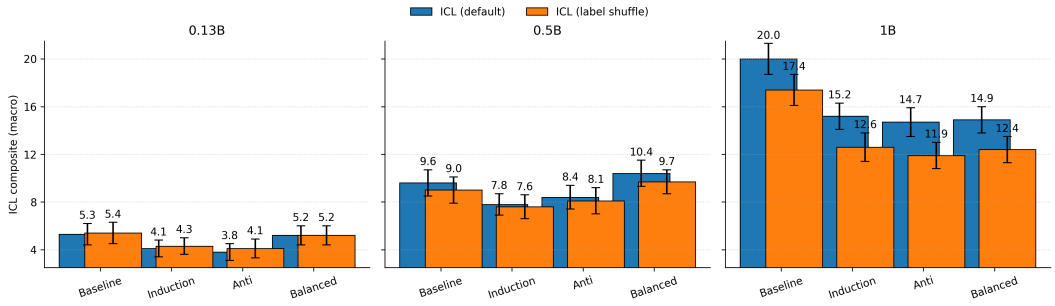

Figure 6: Function-probe suite of Todd et al. (2024) - ICL Composite (macro). Three panels (0.13B, 0.5B, 1B). For each model, bars compare *ICL (default - no label shuffle)* vs *ICL (label shuffle)* across four regimes (Baseline, Induction, Anti, Balanced). Error bars show ± 1 s.d.

2021), and (ii) the ability to override priors and follow contradictory, flipped labels emerges with scale (Wei et al., 2023).

Decision-Rule Sensitivity - HITS@k ($k \in \{1, 3\}$): Following common practice for function-probe tasks in the Todd et al. (2024) suite-which reports HITS@3 (top-3 token accuracy)-we compare our primary decision rule (HITS@1) with HITS@3. ICL performance is summarized in Figure 7, and per-task HITS@3 accuracies are listed in Table 11. While HITS@3 increases absolute scores across the board, the relative ordering and gaps between variants remain effectively unchanged.

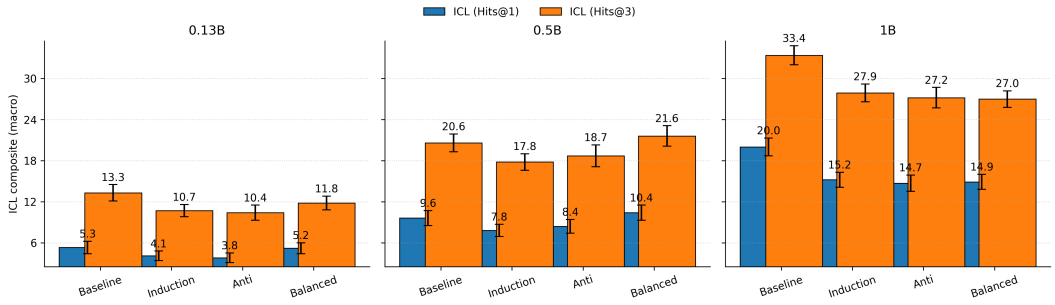

Figure 7: Function-probe suite of Todd et al. (2024) - ICL Composite (macro). Three panels (0.13B, 0.5B, 1B). For each model, bars compare *ICL (HITS@1)* vs *ICL (HITS@3)* across four regimes (Baseline, Induction, Anti, Balanced). Error bars show ± 1 s.d.

E Induction Head Ablation

We quantify how much the in-context learning (ICL) composite depends on the model's most induction-like attention heads by ablating them at evaluation time and comparing the drop to ablating an equal number of random heads.

Selecting induction heads: For each model, we compute a per-head *copy score* exactly as in Section B.2 and select the top 2% per layer for ablation.

Ablation mechanism (value-stream zeroing): At inference, for a chosen set of heads $\mathcal{S}_\ell$ in layer ℓ, we zero their value-stream contribution before the output projection:

$$\tilde{Z}^{(\ell)} \;=\; \big[\, QKV^{(1)} \,\|\, \ldots \,\|\, \underbrace{0}_{h\in\mathcal{S}_\ell} \,\|\, \ldots \,\|\, QKV^{(H)} \,\big], \qquad \text{attn\_out}^{(\ell)} \;=\; \tilde{Z}^{(\ell)} W_O^{(\ell)}.$$

Queries/keys/softmax are unchanged; only the selected heads' post-attention vectors are set to zero. This follows common practice in mechanistic interpretability and avoids softmax renormalization artifacts. We compare two conditions:

- **Induct-head ablation:** zero the per-layer top-2% induction heads defined above.
- **Random-head ablation:** zero the same count of uniformly random heads per layer.

We evaluate the same prompts, shots, and metrics as in the main text (Section 5.1): the macro-averaged ICL composite aggregates task scores (e.g., HITS@1 unless otherwise specified). For each model-curriculum pair we report (i) the clean score, and (ii) the percent change under each ablation relative to its own clean run:

$$\Delta_{\text{induct}} = 100 \times \frac{\text{ICL}_{\text{induct-abl}} - \text{ICL}_{\text{clean}}}{\text{ICL}_{\text{clean}}}, \qquad \Delta_{\text{rand}} = 100 \times \frac{\text{ICL}_{\text{rand-abl}} - \text{ICL}_{\text{clean}}}{\text{ICL}_{\text{clean}}}.$$

Figure 8 shows the ICL composite for clean vs. ablations across scales and curricula; per-task deltas are in Table 12.

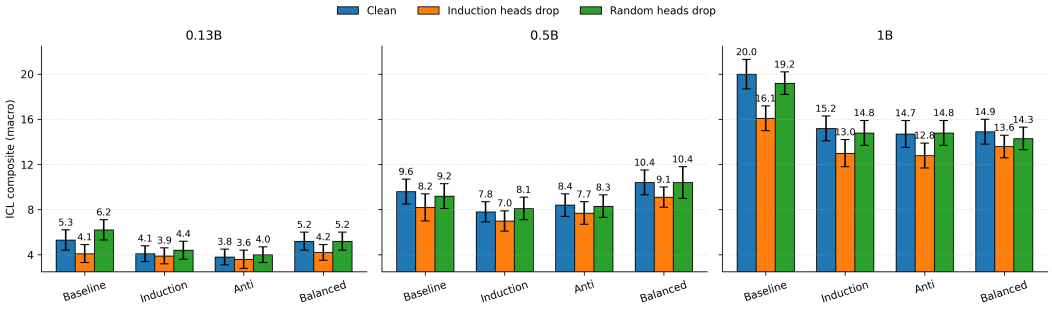

Figure 8: **Function-probe suite of Todd et al. (2024) - ICL composite under clean, induct-head ablation, and random-head ablation.** Three panels (0.13B, 0.5B, 1B), across four regimes (Baseline, Induction, Anti, Balanced). Error bars show ± 1 s.d.

Table 5: Benchmarks, evaluation metrics, and shot counts used to compute the ICL composite in Section 5.1.

Benchmark / Tasks	**Metric**	**Shots**	**Notes**
MMLU (Hendrycks et al., 2021)	Acc	3	57 subject areas; standard 5-shot setup.
Winogrande (Sakaguchi et al., 2019)	Acc	3	Commonsense coreference.
CommonSenseQA (Talmor et al., 2019)	Acc	3	Multiple choice commonsense.
PIQA (Bisk et al., 2020)	Acc	3	Physical commonsense.
HellaSwag (Zellers et al., 2019)	Acc	3	Story completion.
TriviaQA-Wiki (Joshi et al., 2017)	EM	3	Open-domain QA, Wikipedia evidence.
BBH (CoT) (Suzgun et al., 2022)	EM	3	Few hard tasks with chain-of-thought prompts.
OpenBookQA (Mihaylov et al., 2018)	Acc	3	Elementary science QA.
ARC-Challenge (Clark et al., 2018)	Acc	3	Difficult science questions.
GPQA (Rein et al., 2023)	Acc	3	Graduate-level QA.
GSM-8K (Cobbe et al., 2021)	EM	3	Math word problems with short CoT.
MathQA (Amini et al., 2019)	Acc	3	Programmatic math QA.
BoolQ (Clark et al., 2019)	Acc	3	Yes/No reading comprehension.
LAMBADA (OpenAI) (Paperno et al., 2016)	Acc	3	Cloze final-word prediction.
From Todd et al. (2024) function-probe suite:			
`capitalize`	HITS@1 Acc	10	Convert the entire input string to uppercase (e.g., "hello" → "HELLO").
`capitalize_first_letter`	HITS@1 Acc	10	Uppercase the first character only; leave the rest unchanged ("alpha" → "Alpha").
`capitalize_last_letter`	HITS@1 Acc	10	Uppercase the final character only ("gamma" → "gammA").
`lowercase_first_letter`	HITS@1 Acc	10	Lowercase the first character only ("Alpha" → "alpha").
`lowercase_last_letter`	HITS@1 Acc	10	Lowercase the final character only ("GammA" → "Gamma").
`next_capital_letter`	HITS@1 Acc	10	Map an uppercase letter to its successor in the alphabet (e.g., `A`→`B`; wraparound optional).
`next_item`	HITS@1 Acc	10	Given an item from an ordered category (day, month, letter, number word), output the next item ("Monday" → "Tuesday").
`prev_item`	HITS@1 Acc	10	As above, but return the previous item ("Tuesday" → "Monday"; wraparound for cyclic lists).
`word_length`	HITS@1 Acc	10	Return the number of characters in the input word ("token" → `5`).
`alphabetically_first_3`	HITS@1 Acc	10	From a list of 3 strings, choose the alphabetically earliest.
`alphabetically_first_5`	HITS@1 Acc	10	From a list of 5 strings, choose the alphabetically earliest.
`alphabetically_last_3`	HITS@1 Acc	10	From a list of 3 strings, choose the alphabetically latest.
`alphabetically_last_5`	HITS@1 Acc	10	From a list of 5 strings, choose the alphabetically latest.
`choose_first_of_3`	HITS@1 Acc	10	From a list of 3 items, select the first item by position.
`choose_first_of_5`	HITS@1 Acc	10	From a list of 5 items, select the first item by position.
`choose_last_of_3`	HITS@1 Acc	10	From a list of 3 items, select the last item by position.
`choose_last_of_5`	HITS@1 Acc	10	From a list of 5 items, select the last item by position.
`choose_middle_of_3`	HITS@1 Acc	10	From a list of 3 items, select the middle item by position.
`choose_middle_of_5`	HITS@1 Acc	10	From a list of 5 items, select the middle item by position.

Table 6: Span-length sweep at **0.13B** on THE PILE. All curricula are linearly annealed over the full training budget with initial mix of 25%. Results are averaged over six seeds. Evaluation is 5-shot. We report per-task accuracies, the macro ICL composite, and held-out perplexity (PPL).

	Baseline	**Induction**			**Anti-induction**			**Balanced**		
	-	5	20	500	5	20	500	5	20	500
MMLU ↑	25.2 ± 0.3	25.3 ± 0.5	25.1 ± 0.4	25.3 ± 0.5	25.3 ± 0.4	25.1 ± 0.5	24.8 ± 0.5	25.2 ± 0.4	24.8 ± 0.3	25.1 ± 0.2
ARC-Challenge ↑	18.1 ± 0.6	18.7 ± 0.4	18.6 ± 1.3	18.1 ± 0.6	18.5 ± 0.7	18.1 ± 0.4	17.6 ± 0.6	18.6 ± 0.2	18.5 ± 0.6	17.6 ± 0.4
BoolQ ↑	52.8 ± 4.6	46.2 ± 5.2	53.5 ± 5.9	53.4 ± 3.7	50.8 ± 6.8	54.5 ± 1.4	53.4 ± 2.9	51.2 ± 2.5	50.1 ± 3.5	54.7 ± 4.9
LAMBADA ↑	7.6 ± 0.7	6.7 ± 0.6	6.4 ± 0.6	6.8 ± 0.6	6.4 ± 0.5	6.7 ± 0.5	6.2 ± 0.2	7.0 ± 0.1	6.9 ± 0.4	6.5 ± 0.5
PIQA ↑	56.6 ± 0.5	56.5 ± 0.6	55.8 ± 0.5	55.5 ± 0.2	55.9 ± 0.3	55.9 ± 0.6	56.4 ± 0.8	56.0 ± 0.6	55.8 ± 0.5	56.0 ± 0.5
ICL composite (macro) ↑	32.1 ± 0.9	30.7 ± 2.4	31.9 ± 1.1	31.8 ± 1.7	31.6 ± 1.2	32.1 ± 0.3	31.7 ± 1.4	31.4 ± 3.1	31.2 ± 0.7	32.0 ± 2.2
PPL ↓	21.8	23.8	23.9	24.0	23.8	24.0	24.5	23.8	24.0	24.2

Table 7: Initial mix-ratio sweep at **0.13B** on THE PILE. All curricula are linearly annealed over the full training budget with span fixed at $L = 20$. Results are averaged over six seeds. Evaluation is 5-shot. We report per-task accuracies, the macro ICL composite, and held-out perplexity (PPL).

	Baseline	**Induction**			**Anti-induction**			**Balanced**		
	-	25%	50%	100%	25%	50%	100%	25%	50%	100%
MMLU ↑	25.2 ± 0.26	25.1 ± 0.38	25.0 ± 0.33	24.9 ± 0.33	25.1 ± 0.48	25.2 ± 0.40	24.9 ± 0.41	24.8 ± 0.29	25.0 ± 0.27	24.6 ± 0.38
ARC-Challenge ↑	18.1 ± 0.64	18.6 ± 1.28	18.1 ± 0.65	17.9 ± 0.89	18.1 ± 0.42	18.0 ± 0.47	17.5 ± 0.91	18.5 ± 0.58	18.1 ± 0.44	17.8 ± 0.52
BoolQ ↑	52.8 ± 4.64	53.5 ± 5.92	49.6 ± 6.92	51.8 ± 4.51	54.5 ± 1.36	47.8 ± 6.78	51.1 ± 2.87	50.1 ± 3.52	46.9 ± 4.68	51.8 ± 5.37
LAMBADA ↑	7.6 ± 0.69	6.4 ± 0.60	5.6 ± 0.50	4.7 ± 0.50	6.7 ± 0.45	5.6 ± 0.51	4.4 ± 0.45	6.9 ± 0.43	5.9 ± 0.66	4.6 ± 0.38
PIQA ↑	56.6 ± 0.49	55.8 ± 0.48	55.4 ± 0.27	54.9 ± 0.49	55.9 ± 0.55	55.4 ± 0.37	55.2 ± 0.55	55.8 ± 0.50	55.8 ± 0.72	54.4 ± 0.45
ICL composite (macro) ↑	32.06 ± 0.89	31.88 ± 1.08	30.76 ± 1.48	30.83 ± 0.98	32.06 ± 0.25	30.40 ± 1.40	30.62 ± 0.66	31.22 ± 0.69	30.34 ± 0.92	30.64 ± 1.10
PPL ↓	21.8	23.9	26.0	31.4	24.0	26.4	32.9	24.0	26.2	32.8

Table 8: Results across model scales (0.13B, 0.5B, 1B) on THE PILE at iso-FLOPs. Copy snippets use span L=20. Evaluation is few-shot: 3-shot for standard LM benchmarks, and 10-shot for function-style probes. We report per-task accuracy (or EM where standard), averaged over three seeds, and the ICL composite (macro-average across tasks). Higher is better.

	Baseline			**Induction**			**Anti-induction**			**Balanced**		
	0.13B	0.5B	1B	0.13B	0.5B	1B	0.13B	0.5B	1B	0.13B	0.5B	1B
MMLU	26.7 ± 0.1	27.5 ± 0.4	27.7 ± 0.0	25.9 ± 0.0	27.4 ± 0.0	26.6 ± 0.0	27.1 ± 0.0	26.8 ± 0.0	27.2 ± 0.1	26.2 ± 0.1	27.1 ± 0.2	27.1 ± 0.0
Winogrande	50.4 ± 0.6	50.8 ± 1.4	49.8 ± 1.1	47.0 ± 0.9	50.5 ± 1.1	51.1 ± 0.8	51.2 ± 0.9	50.1 ± 1.0	49.8 ± 1.3	50.9 ± 1.6	50.9 ± 0.4	51.0 ± 1.2
CommonSenseQA	20.8 ± 1.2	20.0 ± 1.1	21.2 ± 0.9	20.3 ± 0.3	20.5 ± 0.9	20.5 ± 0.8	20.8 ± 0.3	20.0 ± 1.2	20.0 ± 0.4	20.6 ± 0.7	20.5 ± 0.3	20.4 ± 0.4
PIQA	56.6 ± 0.3	58.5 ± 1.2	59.2 ± 0.5	55.0 ± 0.2	58.6 ± 0.1	58.4 ± 0.3	56.1 ± 0.2	56.9 ± 0.3	58.9 ± 0.6	55.5 ± 0.7	57.2 ± 0.6	58.4 ± 0.3
HellaSwag	26.5 ± 0.1	27.1 ± 0.4	27.8 ± 0.1	26.3 ± 0.1	26.5 ± 0.1	27.2 ± 0.1	26.4 ± 0.1	26.8 ± 0.1	27.3 ± 0.1	26.2 ± 0.1	26.5 ± 0.1	27.3 ± 0.1
TriviaQA-Wiki	0.1 ± 0.0	0.2 ± 0.0	0.4 ± 0.0	0.1 ± 0.0	0.1 ± 0.0	0.3 ± 0.0	0.1 ± 0.0	0.1 ± 0.0	0.3 ± 0.0	0.1 ± 0.0	0.1 ± 0.0	0.3 ± 0.0
BBH (CoT)	0.1 ± 0.0	1.5 ± 0.2	2.8 ± 0.0	0.3 ± 0.0	1.6 ± 0.1	1.2 ± 0.1	0.8 ± 0.1	0.1 ± 0.0	0.6 ± 0.0	0.1 ± 0.0	2.2 ± 0.0	4.2 ± 0.0
OpenBookQA	14.3 ± 0.6	14.0 ± 1.6	15.9 ± 1.1	13.9 ± 0.8	15.3 ± 0.1	15.3 ± 0.4	14.7 ± 0.7	13.9 ± 1.3	15.6 ± 0.4	13.1 ± 0.1	13.6 ± 1.0	16.5 ± 0.5
ARC-Challenge	18.6 ± 0.6	18.4 ± 1.1	18.2 ± 0.6	18.3 ± 0.3	18.5 ± 0.7	18.1 ± 0.4	17.6 ± 0.4	17.8 ± 0.4	19.0 ± 0.4	17.1 ± 0.8	17.9 ± 0.4	17.9 ± 0.3
GPQA	25.2 ± 2.2	26.1 ± 2.1	25.2 ± 2.0	23.7 ± 2.3	25.2 ± 1.7	24.3 ± 1.5	23.9 ± 2.0	24.9 ± 1.4	24.1 ± 1.1	24.1 ± 2.2	22.8 ± 0.8	24.6 ± 0.8
GSM-8K	1.5 ± 0.4	1.5 ± 0.3	1.7 ± 0.2	1.1 ± 0.3	1.5 ± 0.3	1.5 ± 0.2	1.4 ± 0.2	1.2 ± 0.1	1.6 ± 0.1	1.1 ± 0.4	1.7 ± 0.2	1.4 ± 0.2
MathQA	20.5 ± 0.4	20.9 ± 0.7	20.5 ± 0.7	19.9 ± 0.6	20.3 ± 0.2	20.7 ± 0.6	20.2 ± 0.3	20.4 ± 0.4	21.1 ± 0.2	21.0 ± 0.7	20.8 ± 0.4	21.0 ± 0.1
BoolQ	48.8 ± 0.5	53.4 ± 0.9	54.7 ± 0.2	49.1 ± 0.7	60.5 ± 0.3	57.0 ± 0.9	49.1 ± 0.8	52.2 ± 2.2	52.7 ± 0.3	51.4 ± 0.5	57.1 ± 1.0	58.1 ± 0.4
LAMBADA (OpenAI)	8.2 ± 0.2	11.0 ± 0.4	13.2 ± 0.1	5.5 ± 0.1	8.6 ± 0.1	12.2 ± 0.2	5.2 ± 0.2	8.4 ± 0.3	12.2 ± 0.2	6.0 ± 0.2	8.2 ± 0.2	12.0 ± 0.3
ICL composite (macro) ↑	22.7 ± 0.5	23.6 ± 0.8	24.2 ± 0.5	21.9 ± 0.5	23.9 ± 0.4	23.9 ± 0.5	22.5 ± 0.4	22.8 ± 0.6	23.6 ± 0.4	22.4 ± 0.6	23.3 ± 0.4	24.3 ± 0.3
alphabetically_first_3	4.9 ± 0.6	9.4 ± 0.6	19.7 ± 0.9	4.6 ± 0.6	7.3 ± 0.3	15.1 ± 0.9	3.3 ± 0.5	8.5 ± 0.9	14.4 ± 1.5	4.8 ± 0.6	11.5 ± 0.6	15.3 ± 1.0
alphabetically_first_5	4.0 ± 0.6	6.7 ± 0.8	12.4 ± 1.4	4.2 ± 0.8	6.5 ± 1.0	10.9 ± 0.9	2.8 ± 0.7	7.4 ± 0.6	8.4 ± 1.1	3.9 ± 1.0	8.2 ± 0.8	10.2 ± 0.7
alphabetically_last_3	3.4 ± 0.5	10.2 ± 0.9	20.8 ± 0.6	2.4 ± 0.5	7.7 ± 0.2	15.8 ± 1.0	1.9 ± 0.6	8.0 ± 0.9	13.3 ± 0.8	3.9 ± 0.5	10.9 ± 0.5	15.3 ± 1.3
alphabetically_last_5	2.5 ± 0.7	6.0 ± 1.3	9.9 ± 0.8	1.6 ± 0.3	5.5 ± 0.4	8.5 ± 0.3	1.8 ± 0.4	6.1 ± 0.8	7.8 ± 0.5	2.5 ± 0.8	6.7 ± 0.6	9.3 ± 0.4
capitalize	8.0 ± 1.0	20.7 ± 1.4	54.8 ± 2.1	3.3 ± 0.3	13.2 ± 1.3	33.4 ± 1.3	3.7 ± 0.1	13.5 ± 1.3	39.2 ± 2.7	6.0 ± 1.6	14.7 ± 1.3	33.6 ± 2.1
capitalize_first_letter	10.1 ± 1.2	12.5 ± 1.8	28.6 ± 1.1	5.3 ± 1.0	13.4 ± 1.7	13.7 ± 1.2	5.2 ± 0.3	11.2 ± 1.2	17.4 ± 0.8	8.9 ± 0.7	10.0 ± 1.1	20.4 ± 1.2
capitalize_last_letter	4.8 ± 1.3	9.6 ± 1.0	8.3 ± 1.2	8.6 ± 1.1	7.5 ± 1.8	8.6 ± 0.9	9.1 ± 1.4	9.3 ± 1.2	7.3 ± 1.5	5.5 ± 0.7	5.8 ± 1.4	6.7 ± 0.7
choose_first_of_3	10.3 ± 2.3	25.5 ± 1.8	69.4 ± 1.8	6.1 ± 0.9	19.0 ± 1.7	52.4 ± 2.0	4.1 ± 0.7	19.1 ± 1.8	46.0 ± 2.0	11.3 ± 0.7	35.2 ± 1.7	54.1 ± 1.7
choose_first_of_5	8.7 ± 1.3	19.7 ± 1.9	55.5 ± 1.3	4.9 ± 0.7	15.3 ± 0.9	42.6 ± 3.0	3.6 ± 0.7	16.2 ± 1.5	32.7 ± 1.6	7.9 ± 1.0	28.2 ± 2.4	42.1 ± 1.4
choose_last_of_3	2.0 ± 0.4	3.2 ± 0.2	4.4 ± 1.0	1.4 ± 0.4	2.8 ± 0.3	5.4 ± 0.9	1.4 ± 0.5	3.0 ± 0.5	5.0 ± 0.5	1.7 ± 0.3	3.0 ± 0.5	5.2 ± 0.3
choose_last_of_5	1.5 ± 0.3	2.9 ± 0.6	3.9 ± 1.1	1.7 ± 0.5	2.4 ± 0.4	4.6 ± 0.6	1.1 ± 0.4	2.9 ± 0.5	5.6 ± 0.5	1.5 ± 0.3	2.6 ± 0.4	5.1 ± 0.4
choose_middle_of_3	1.7 ± 0.6	3.3 ± 0.5	4.2 ± 0.5	2.1 ± 0.8	2.2 ± 0.3	6.0 ± 1.0	1.3 ± 0.5	3.1 ± 0.2	5.0 ± 0.3	1.7 ± 0.7	3.4 ± 0.7	4.9 ± 0.7
choose_middle_of_5	1.6 ± 0.3	3.0 ± 0.6	2.7 ± 0.4	1.6 ± 0.2	2.1 ± 0.3	3.1 ± 0.6	1.7 ± 0.4	2.9 ± 0.7	3.9 ± 0.7	1.7 ± 0.4	2.3 ± 0.6	4.7 ± 0.6
lowercase_first_letter	5.5 ± 0.8	8.4 ± 0.9	28.5 ± 2.2	4.1 ± 0.9	6.1 ± 1.2	20.1 ± 1.6	4.7 ± 0.7	6.5 ± 0.6	20.6 ± 1.1	2.2 ± 0.6	8.8 ± 0.7	13.3 ± 0.8
lowercase_last_letter	11.1 ± 0.8	7.7 ± 0.7	10.5 ± 1.1	3.6 ± 0.7	8.0 ± 0.7	9.6 ± 1.0	7.4 ± 1.2	8.9 ± 1.0	13.3 ± 0.5	7.8 ± 1.1	10.9 ± 1.5	8.9 ± 1.2
next_capital_letter	4.9 ± 1.1	4.2 ± 0.9	2.4 ± 0.8	3.9 ± 0.3	4.2 ± 1.0	3.6 ± 0.7	4.7 ± 0.8	4.1 ± 0.7	3.1 ± 0.9	4.8 ± 0.9	3.5 ± 0.9	4.2 ± 1.1
next_item	3.4 ± 2.2	8.6 ± 2.5	16.8 ± 2.1	2.9 ± 1.9	5.7 ± 1.3	11.8 ± 1.2	1.3 ± 0.9	7.8 ± 1.1	11.8 ± 2.5	6.3 ± 0.8	9.0 ± 1.6	9.4 ± 1.7
prev_item	2.5 ± 0.8	7.7 ± 1.6	15.1 ± 2.3	2.0 ± 0.8	5.9 ± 0.7	10.3 ± 1.0	1.4 ± 0.5	6.6 ± 2.5	11.4 ± 2.5	5.7 ± 1.3	8.4 ± 1.2	7.7 ± 2.2
word_length	9.9 ± 1.0	13.3 ± 0.9	12.8 ± 1.1	13.4 ± 0.8	14.0 ± 1.0	13.3 ± 0.8	12.0 ± 1.3	14.3 ± 0.6	13.6 ± 1.6	10.8 ± 1.1	14.7 ± 1.8	12.6 ± 0.7
ICL composite (macro) ↑	5.3 ± 0.9	9.6 ± 1.1	20.0 ± 1.3	4.1 ± 0.7	7.8 ± 0.9	15.2 ± 1.1	3.8 ± 0.7	8.4 ± 1.0	14.7 ± 1.2	5.2 ± 0.8	10.4 ± 1.1	14.9 ± 1.1

Table 9: Results across model scales (0.13B, 0.5B, 1B) on THE PILE at iso-FLOPs. Copy snippets use span L=20. Evaluation is few-shot: 1-shot for both standard LM benchmarks, and function-style probes. We report per-task accuracy (or EM where standard), averaged over three seeds, and the ICL composite (macro-average across tasks). Higher is better.

	Baseline			**Induction**			**Anti-induction**			**Balanced**		
	0.13B	0.5B	1B	0.13B	0.5B	1B	0.13B	0.5B	1B	0.13B	0.5B	1B
MMLU	25.8 ± 0.0	25.2 ± 0.3	26.8 ± 0.0	25.8 ± 0.0	24.4 ± 0.3	26.4 ± 0.0	25.8 ± 0.0	24.7 ± 0.3	26.8 ± 0.0	25.9 ± 0.0	24.3 ± 0.2	27.3 ± 0.0
Winogrande	49.8 ± 0.8	50.3 ± 0.5	49.6 ± 0.4	48.9 ± 0.3	50.2 ± 0.3	50.6 ± 0.4	50.9 ± 1.2	50.4 ± 0.8	49.3 ± 0.9	50.8 ± 0.3	52.0 ± 0.4	51.0 ± 0.0
CommonSenseQA	20.9 ± 0.9	20.6 ± 1.0	20.5 ± 0.5	20.8 ± 0.8	20.6 ± 0.9	20.6 ± 0.6	20.9 ± 0.8	20.6 ± 1.0	20.7 ± 0.1	21.0 ± 0.8	20.7 ± 0.9	20.6 ± 0.6
PIQA	56.8 ± 0.4	58.7 ± 0.8	59.9 ± 0.4	55.4 ± 0.2	58.8 ± 0.2	58.3 ± 0.3	55.9 ± 0.1	57.4 ± 0.5	59.0 ± 1.1	55.4 ± 0.9	57.3 ± 0.3	58.1 ± 0.2
HellaSwag	26.4 ± 0.1	27.0 ± 0.1	27.8 ± 0.1	26.2 ± 0.1	26.7 ± 0.0	27.3 ± 0.1	26.3 ± 0.1	26.7 ± 0.2	27.3 ± 0.1	26.2 ± 0.1	26.6 ± 0.1	27.2 ± 0.2
TriviaQA-Wiki	0.1 ± 0.0	0.1 ± 0.0	0.3 ± 0.0	0.1 ± 0.0	0.1 ± 0.0	0.1 ± 0.0	0.1 ± 0.0	0.1 ± 0.0	0.1 ± 0.0	0.1 ± 0.0	0.1 ± 0.0	0.2 ± 0.0
BBH (CoT)	0.0 ± 0.0	0.6 ± 0.0	3.4 ± 0.0	0.1 ± 0.02	2.0 ± 0.0	4.3 ± 0.0	0.4 ± 0.00	0.1 ± 0.0	0.6 ± 0.1	0.4 ± 0.00	1.8 ± 1.1	2.8 ± 0.0
OpenBookQA	14.3 ± 0.5	15.6 ± 0.7	15.8 ± 0.5	14.3 ± 0.2	14.5 ± 0.8	15.5 ± 0.5	13.0 ± 0.0	14.7 ± 0.2	16.7 ± 0.7	13.3 ± 0.1	13.9 ± 0.1	15.6 ± 1.2
ARC-Challenge	18.4 ± 0.2	19.0 ± 0.4	18.1 ± 0.1	18.7 ± 0.4	18.2 ± 0.1	18.3 ± 0.2	17.7 ± 0.3	17.8 ± 0.2	18.4 ± 0.5	17.5 ± 0.4	17.8 ± 0.4	17.7 ± 0.7
GPQA	24.8 ± 0.6	25.0 ± 1.0	26.2 ± 2.5	25.0 ± 0.8	24.4 ± 1.3	25.2 ± 0.6	25.1 ± 1.1	25.9 ± 1.2	25.7 ± 1.2	25.5 ± 0.3	24.2 ± 2.1	26.0 ± 2.0
GSM-8K	1.3 ± 0.1	1.9 ± 0.3	1.3 ± 0.1	1.5 ± 0.6	2.2 ± 0.3	1.5 ± 0.2	1.3 ± 0.5	1.8 ± 0.2	1.6 ± 0.3	1.1 ± 0.1	2.0 ± 0.3	1.5 ± 0.2
MathQA	20.7 ± 0.3	20.4 ± 0.2	20.7 ± 0.3	20.3 ± 0.5	20.2 ± 0.3	21.1 ± 0.3	20.1 ± 0.1	20.3 ± 0.1	20.8 ± 0.7	20.6 ± 0.4	20.2 ± 0.3	21.0 ± 1.0
BoolQ	53.2 ± 0.8	53.4 ± 0.8	54.2 ± 0.3	53.2 ± 0.8	57.6 ± 1.1	56.0 ± 0.2	50.8 ± 0.8	53.0 ± 0.7	54.1 ± 0.1	53.1 ± 0.8	53.1 ± 0.7	55.2 ± 0.4
LAMBADA	9.5 ± 0.1	11.9 ± 0.1	15.1 ± 0.1	6.5 ± 0.1	9.9 ± 0.2	13.4 ± 0.2	5.9 ± 0.2	9.6 ± 0.3	13.5 ± 0.2	7.0 ± 0.1	9.2 ± 0.1	13.8 ± 0.5
ICL composite (macro)	23.0 ± 0.3	23.6 ± 0.4	24.3 ± 0.4	22.6 ± 0.3	23.6 ± 0.4	24.2 ± 0.3	22.4 ± 0.4	23.1 ± 0.4	23.9 ± 0.4	22.7 ± 0.3	23.1 ± 0.5	24.1 ± 0.5
alphabetically_first_3	2.6 ± 0.6	3.0 ± 0.7	13.2 ± 1.3	3.3 ± 0.7	4.8 ± 0.6	8.9 ± 0.8	1.9 ± 0.4	3.5 ± 0.8	5.8 ± 1.0	3.6 ± 0.7	4.4 ± 0.4	8.5 ± 0.8
alphabetically_first_5	2.7 ± 0.4	3.3 ± 0.5	8.9 ± 0.5	3.3 ± 0.1	4.3 ± 0.2	7.5 ± 0.4	2.0 ± 0.3	3.7 ± 0.8	4.4 ± 0.8	2.2 ± 0.4	3.1 ± 0.6	6.8 ± 1.1
alphabetically_last_3	2.1 ± 0.5	2.9 ± 0.5	13.3 ± 1.2	3.1 ± 0.4	4.3 ± 0.9	9.2 ± 1.0	1.9 ± 0.4	2.9 ± 0.3	6.8 ± 0.6	4.5 ± 0.3	3.8 ± 0.5	10.6 ± 0.9
alphabetically_last_5	1.6 ± 0.5	2.8 ± 0.4	8.5 ± 0.9	1.9 ± 0.6	3.2 ± 0.4	6.0 ± 0.3	1.4 ± 0.4	2.3 ± 0.5	4.5 ± 0.4	2.2 ± 0.4	3.0 ± 0.8	6.8 ± 0.6
capitalize	2.9 ± 0.6	1.5 ± 0.4	4.4 ± 0.7	1.8 ± 0.3	5.1 ± 0.8	2.6 ± 0.8	1.8 ± 0.2	2.5 ± 0.5	4.9 ± 0.6	2.7 ± 0.4	3.1 ± 0.5	3.7 ± 1.1
capitalize_first_letter	4.1 ± 1.1	3.0 ± 0.9	3.4 ± 0.7	3.5 ± 1.0	5.6 ± 1.4	4.0 ± 1.2	3.5 ± 1.0	4.7 ± 1.2	4.0 ± 0.9	4.4 ± 1.0	4.9 ± 0.8	3.5 ± 1.1
capitalize_last_letter	9.0 ± 0.7	7.4 ± 0.4	5.6 ± 0.9	9.1 ± 0.8	6.0 ± 0.7	8.4 ± 0.4	9.2 ± 0.8	8.7 ± 0.9	8.4 ± 0.8	8.7 ± 0.7	8.8 ± 0.8	8.8 ± 0.5
choose_first_of_3	5.6 ± 0.5	6.7 ± 1.0	37.0 ± 1.2	5.5 ± 0.8	7.4 ± 1.3	25.1 ± 2.1	1.5 ± 0.4	6.0 ± 1.1	14.6 ± 1.0	8.9 ± 1.0	7.2 ± 0.8	26.1 ± 1.8
choose_first_of_5	5.9 ± 0.4	6.9 ± 0.8	32.0 ± 1.2	3.9 ± 0.8	5.6 ± 0.6	24.9 ± 1.9	1.1 ± 0.3	6.1 ± 0.8	12.5 ± 1.9	5.3 ± 0.3	4.8 ± 0.6	23.8 ± 1.4
choose_last_of_3	0.8 ± 0.3	1.1 ± 0.3	3.7 ± 0.6	1.3 ± 0.4	1.9 ± 0.3	2.4 ± 0.5	1.2 ± 0.4	1.3 ± 0.7	2.0 ± 0.4	0.7 ± 0.2	1.9 ± 0.7	3.7 ± 0.3
choose_last_of_5	0.9 ± 0.3	1.1 ± 0.4	2.4 ± 0.4	1.4 ± 0.3	1.5 ± 0.3	2.0 ± 0.4	0.9 ± 0.3	1.3 ± 0.4	1.9 ± 0.6	0.6 ± 0.2	1.3 ± 0.4	3.1 ± 0.6
choose_middle_of_3	0.7 ± 0.3	1.1 ± 0.4	3.5 ± 0.6	0.9 ± 0.1	1.6 ± 0.4	2.5 ± 0.6	0.7 ± 0.2	1.1 ± 0.1	1.9 ± 0.5	0.6 ± 0.1	1.1 ± 0.2	3.6 ± 0.4
choose_middle_of_5	0.9 ± 0.4	1.4 ± 0.5	2.3 ± 0.5	1.2 ± 0.3	1.4 ± 0.2	2.2 ± 0.5	1.2 ± 0.3	1.3 ± 0.5	1.6 ± 0.4	0.8 ± 0.4	1.5 ± 0.7	3.0 ± 0.6
lowercase_first_letter	4.9 ± 0.7	3.7 ± 0.7	4.0 ± 0.3	4.0 ± 0.7	3.9 ± 0.6	4.6 ± 0.8	2.6 ± 0.5	4.7 ± 0.7	4.7 ± 0.8	2.3 ± 0.5	4.7 ± 0.7	4.4 ± 0.8
lowercase_last_letter	10.6 ± 1.2	9.3 ± 1.2	9.5 ± 1.2	6.6 ± 0.9	7.7 ± 1.3	10.6 ± 1.2	7.6 ± 0.5	10.6 ± 1.2	10.6 ± 1.2	8.7 ± 1.3	10.6 ± 1.2	10.3 ± 1.2
next_capital_letter	4.5 ± 0.3	3.8 ± 0.6	3.6 ± 1.0	4.6 ± 0.5	3.9 ± 0.4	4.5 ± 0.4	4.4 ± 0.4	4.7 ± 0.1	4.1 ± 0.5	4.1 ± 0.4	4.5 ± 0.4	4.6 ± 0.5
next_item	2.5 ± 0.4	2.0 ± 1.7	9.7 ± 1.0	3.9 ± 0.8	5.1 ± 1.4	5.1 ± 1.2	1.5 ± 1.1	2.8 ± 1.1	3.5 ± 0.8	4.4 ± 2.1	4.2 ± 1.1	3.4 ± 1.5
prev_item	2.5 ± 1.2	2.3 ± 1.7	9.2 ± 1.6	3.0 ± 1.1	5.1 ± 1.6	5.7 ± 2.0	1.8 ± 0.7	3.3 ± 1.9	3.4 ± 1.9	4.6 ± 0.7	3.0 ± 1.5	3.8 ± 1.3
word_length	13.8 ± 1.9	13.7 ± 1.7	12.7 ± 2.2	12.7 ± 1.5	13.4 ± 2.1	13.6 ± 1.5	12.5 ± 1.6	13.9 ± 1.7	13.9 ± 1.4	10.6 ± 1.0	13.9 ± 1.7	13.9 ± 1.9
ICL composite (macro) ↑	4.1 ± 0.6	4.1 ± 0.8	9.8 ± 0.9	3.9 ± 0.6	4.8 ± 0.8	7.9 ± 1.0	3.1 ± 0.5	4.5 ± 0.8	6.0 ± 0.9	4.2 ± 0.6	4.7 ± 0.7	8.0 ± 1.0

Table 10: Function-probe suite of Todd et al. (2024) under label-permutation stress (Todd et al. (2024) suite): HITS@1 accuracy on 10-shot prompts with demonstration labels randomly permuted; reported as mean±std across three seeds for 0.13B, 0.5B, and 1B, comparing Baseline, Induction, Anti, and Balanced curricula.

	Baseline			**Induction**			**Anti-induction**			**Balanced**		
	0.13B	0.5B	1B	0.13B	0.5B	1B	0.13B	0.5B	1B	0.13B	0.5B	1B
alphabetically_first_3	4.4 ± 0.4	9.2 ± 0.7	16.6 ± 0.6	4.4 ± 0.3	7.0 ± 0.7	12.3 ± 1.4	3.6 ± 0.5	8.2 ± 0.8	11.0 ± 1.3	4.2 ± 0.7	10.7 ± 1.4	12.5 ± 0.8
alphabetically_first_5	4.1 ± 0.7	7.1 ± 1.1	11.1 ± 0.9	4.2 ± 0.6	5.9 ± 0.4	9.4 ± 0.5	2.6 ± 0.9	7.0 ± 0.9	7.0 ± 0.4	3.5 ± 0.4	7.8 ± 1.0	9.0 ± 0.5
alphabetically_last_3	3.2 ± 0.6	9.7 ± 0.8	16.1 ± 1.6	2.6 ± 0.6	7.3 ± 0.9	12.3 ± 0.6	2.7 ± 1.0	7.4 ± 1.3	10.4 ± 0.9	4.8 ± 0.6	10.7 ± 1.4	13.0 ± 0.6
alphabetically_last_5	2.6 ± 0.3	5.8 ± 0.9	9.5 ± 0.2	1.6 ± 0.3	5.3 ± 0.3	7.8 ± 0.7	1.6 ± 0.5	5.5 ± 0.6	6.4 ± 0.8	2.0 ± 0.2	6.7 ± 0.5	8.5 ± 0.9
capitalize	8.7 ± 0.8	18.2 ± 1.9	49.3 ± 2.9	3.6 ± 1.0	13.3 ± 1.8	29.9 ± 0.8	4.3 ± 0.7	13.5 ± 1.6	34.3 ± 1.4	6.8 ± 0.6	14.5 ± 0.9	31.0 ± 1.9
capitalize_first_letter	10.4 ± 2.1	13.2 ± 1.4	29.0 ± 1.4	6.4 ± 0.4	13.3 ± 0.8	15.2 ± 1.4	6.4 ± 0.9	12.2 ± 1.9	17.5 ± 1.3	9.2 ± 1.5	10.8 ± 2.2	21.2 ± 0.7
capitalize_last_letter	4.7 ± 1.0	8.2 ± 1.0	7.7 ± 0.7	7.9 ± 1.2	6.7 ± 0.8	7.4 ± 1.3	8.9 ± 1.7	8.6 ± 0.9	5.9 ± 1.4	5.2 ± 0.7	5.3 ± 0.9	6.5 ± 1.4
choose_first_of_3	11.2 ± 1.2	21.9 ± 2.1	54.9 ± 2.6	6.9 ± 1.2	19.1 ± 2.5	35.0 ± 2.5	5.2 ± 0.4	19.0 ± 2.0	28.9 ± 0.8	13.4 ± 1.0	32.4 ± 1.1	34.5 ± 1.6
choose_first_of_5	9.3 ± 1.5	17.3 ± 1.6	42.0 ± 2.3	5.6 ± 0.9	15.3 ± 1.8	28.9 ± 2.1	3.6 ± 0.4	16.8 ± 1.9	20.3 ± 1.3	8.5 ± 1.7	23.7 ± 1.9	26.4 ± 1.9
choose_last_of_3	1.6 ± 0.4	2.7 ± 0.6	4.3 ± 0.9	2.1 ± 0.6	2.6 ± 0.4	4.9 ± 0.5	1.3 ± 0.4	2.8 ± 0.3	4.9 ± 1.2	1.3 ± 0.3	3.3 ± 0.7	5.4 ± 0.6
choose_last_of_5	1.7 ± 0.4	2.2 ± 0.6	3.9 ± 0.8	1.9 ± 0.4	2.1 ± 0.3	4.5 ± 0.6	1.1 ± 0.4	2.3 ± 0.6	5.5 ± 0.7	1.2 ± 0.5	2.3 ± 0.8	4.7 ± 0.3
choose_middle_of_3	1.9 ± 0.3	3.5 ± 0.5	4.5 ± 0.9	2.3 ± 0.6	2.8 ± 0.7	5.6 ± 1.1	1.4 ± 0.5	3.0 ± 0.4	4.6 ± 0.3	1.5 ± 0.2	3.1 ± 0.3	5.2 ± 0.8
choose_middle_of_5	1.8 ± 0.7	3.6 ± 0.8	2.9 ± 0.5	1.9 ± 0.3	2.2 ± 0.6	3.3 ± 0.4	1.5 ± 0.6	2.8 ± 0.4	3.9 ± 0.5	1.7 ± 0.2	2.4 ± 0.4	4.6 ± 0.7
lowercase_first_letter	6.7 ± 0.8	9.3 ± 0.6	27.8 ± 1.6	4.9 ± 0.7	6.5 ± 0.4	19.0 ± 1.1	5.4 ± 1.1	7.5 ± 1.1	18.4 ± 1.9	2.5 ± 0.6	10.4 ± 0.9	13.9 ± 1.4
lowercase_last_letter	10.1 ± 1.0	7.5 ± 1.2	8.8 ± 1.9	3.5 ± 1.2	8.0 ± 1.6	8.2 ± 1.2	7.1 ± 0.9	8.4 ± 1.7	12.8 ± 1.8	7.1 ± 0.7	9.5 ± 1.3	7.8 ± 1.5
next_capital_letter	4.3 ± 0.9	4.3 ± 0.5	2.8 ± 0.4	4.2 ± 0.6	3.5 ± 0.6	3.6 ± 0.6	4.7 ± 0.6	4.2 ± 0.7	3.0 ± 0.6	4.3 ± 0.5	3.3 ± 0.6	3.0 ± 0.1
next_item	3.3 ± 1.0	7.3 ± 1.3	15.3 ± 1.8	2.7 ± 0.8	4.7 ± 0.8	10.8 ± 2.2	1.8 ± 1.0	4.9 ± 1.2	9.7 ± 2.7	5.3 ± 1.5	6.6 ± 1.4	7.2 ± 1.0
prev_item	3.2 ± 1.7	6.5 ± 2.3	13.5 ± 1.6	2.5 ± 1.4	5.6 ± 1.4	8.6 ± 1.8	2.3 ± 1.5	4.9 ± 1.1	9.2 ± 1.1	4.8 ± 1.7	6.5 ± 1.4	7.8 ± 1.0
word_length	9.7 ± 0.8	12.6 ± 1.3	11.4 ± 1.8	12.8 ± 1.0	12.9 ± 1.4	12.4 ± 1.1	12.1 ± 1.1	14.5 ± 1.6	13.2 ± 0.2	11.1 ± 0.9	14.3 ± 0.8	12.6 ± 1.0
ICL composite (macro) ↑	5.4 ± 0.9	9.0 ± 1.1	17.4 ± 1.3	4.3 ± 0.7	7.6 ± 1.0	12.6 ± 1.2	4.1 ± 0.8	8.1 ± 1.1	11.9 ± 1.1	5.2 ± 0.8	9.7 ± 1.0	12.4 ± 1.0

Table 11: Function-probe suite of Todd et al. (2024) under decision-rule sensitivity: HITS@3 accuracy on 10-shot prompts, reported as mean±std across three seeds, for 0.13B, 0.5B, and 1B, comparing Baseline, Induction, Anti, and Balanced curricula.

	Baseline			Induction			Anti-induction			Balanced		
	0.13B	0.5B	1B	0.13B	0.5B	1B	0.13B	0.5B	1B	0.13B	0.5B	1B
alphabetically_first_3	8.8 ± 0.8	15.3 ± 0.5	31.0 ± 0.5	8.6 ± 1.3	12.7 ± 0.3	23.0 ± 0.8	7.1 ± 0.3	13.7 ± 0.8	22.6 ± 1.4	9.3 ± 1.2	18.6 ± 0.6	24.1 ± 0.8
alphabetically_first_5	8.6 ± 1.3	13.0 ± 0.5	20.7 ± 1.5	8.3 ± 0.9	12.1 ± 1.0	16.4 ± 0.6	7.4 ± 0.7	13.6 ± 1.3	15.5 ± 1.3	7.8 ± 1.3	13.3 ± 0.6	15.9 ± 0.8
alphabetically_last_3	7.3 ± 0.9	17.4 ± 0.7	30.3 ± 1.0	6.3 ± 0.7	14.3 ± 0.5	24.5 ± 1.1	5.7 ± 0.7	14.6 ± 1.5	22.3 ± 1.5	8.9 ± 0.3	19.1 ± 1.1	24.0 ± 0.9
alphabetically_last_5	5.8 ± 0.8	12.6 ± 1.7	18.6 ± 1.1	4.9 ± 0.8	11.4 ± 0.8	14.6 ± 0.7	4.5 ± 0.5	10.9 ± 1.4	14.0 ± 1.0	5.6 ± 0.8	12.9 ± 0.9	15.6 ± 1.0
capitalize	17.8 ± 1.1	39.7 ± 1.6	73.8 ± 1.4	10.6 ± 0.4	28.5 ± 0.9	57.7 ± 1.3	11.5 ± 1.2	28.9 ± 1.3	60.6 ± 0.8	14.0 ± 2.0	32.2 ± 1.4	56.0 ± 0.8
capitalize_first_letter	25.6 ± 1.6	34.7 ± 1.8	55.2 ± 2.0	17.1 ± 1.1	30.7 ± 1.7	40.1 ± 1.6	19.1 ± 1.5	29.9 ± 1.7	43.5 ± 2.1	22.3 ± 1.7	29.6 ± 1.3	42.0 ± 2.1
capitalize_last_letter	14.1 ± 1.7	25.6 ± 1.7	20.4 ± 2.8	20.0 ± 1.1	18.8 ± 1.9	23.0 ± 2.4	20.8 ± 2.1	23.2 ± 2.8	17.2 ± 1.8	15.6 ± 0.8	15.9 ± 1.7	18.6 ± 2.7
choose_first_of_3	18.3 ± 1.9	38.6 ± 1.9	83.6 ± 0.6	12.9 ± 1.0	27.8 ± 1.7	66.6 ± 1.6	9.8 ± 1.1	28.3 ± 1.2	60.7 ± 0.9	19.5 ± 1.1	50.3 ± 2.1	67.7 ± 1.0
choose_first_of_5	17.1 ± 1.7	30.6 ± 1.9	74.1 ± 1.1	11.3 ± 0.7	24.4 ± 1.6	56.2 ± 1.3	8.0 ± 1.3	26.3 ± 1.7	48.3 ± 1.5	15.4 ± 1.2	41.5 ± 1.8	56.7 ± 1.8
choose_last_of_3	5.1 ± 0.4	8.0 ± 0.6	11.0 ± 1.0	4.5 ± 0.9	8.7 ± 0.7	11.5 ± 1.3	3.9 ± 0.5	7.9 ± 0.6	11.6 ± 0.6	4.0 ± 0.6	8.7 ± 1.2	12.4 ± 0.4
choose_last_of_5	4.0 ± 0.6	7.1 ± 0.7	9.3 ± 1.1	4.9 ± 0.6	7.0 ± 0.8	10.3 ± 0.7	3.5 ± 0.6	7.6 ± 0.8	10.1 ± 0.6	4.1 ± 0.7	6.6 ± 0.4	10.6 ± 1.0
choose_middle_of_3	4.8 ± 1.1	8.7 ± 0.7	12.5 ± 1.0	5.5 ± 0.4	7.7 ± 0.7	13.1 ± 0.7	4.0 ± 0.2	7.8 ± 0.4	10.3 ± 0.7	4.4 ± 0.6	8.1 ± 1.1	11.4 ± 0.7
choose_middle_of_5	4.6 ± 0.7	7.6 ± 0.5	7.7 ± 0.8	4.5 ± 0.2	6.2 ± 0.8	7.4 ± 0.9	4.5 ± 0.9	7.4 ± 1.1	8.4 ± 0.7	4.2 ± 0.8	6.5 ± 0.9	9.3 ± 1.0
lowercase_first_letter	19.4 ± 2.0	28.7 ± 0.9	58.6 ± 2.3	11.4 ± 1.0	22.1 ± 1.4	49.5 ± 1.9	12.4 ± 1.7	22.8 ± 3.2	45.1 ± 2.2	5.5 ± 0.3	30.5 ± 1.6	38.7 ± 0.5
lowercase_last_letter	28.0 ± 1.4	19.4 ± 1.1	23.5 ± 1.2	8.7 ± 1.2	23.1 ± 0.6	26.2 ± 1.3	20.2 ± 1.1	24.0 ± 0.9	29.7 ± 0.9	13.2 ± 1.2	26.8 ± 2.0	22.8 ± 1.8
next_capital_letter	15.0 ± 0.5	13.2 ± 1.2	12.5 ± 0.7	13.2 ± 0.9	12.4 ± 1.8	11.7 ± 1.4	16.0 ± 1.0	13.7 ± 1.4	10.9 ± 2.0	12.5 ± 0.8	11.1 ± 1.4	13.3 ± 1.5
next_item	8.5 ± 2.2	18.7 ± 3.9	29.5 ± 3.2	9.0 ± 1.9	15.8 ± 1.9	23.4 ± 0.8	5.8 ± 2.0	18.2 ± 3.4	25.4 ± 1.9	13.5 ± 1.2	20.5 ± 3.0	20.3 ± 2.1
prev_item	8.4 ± 0.8	15.1 ± 1.4	24.7 ± 2.4	7.6 ± 1.2	14.9 ± 2.1	17.3 ± 1.3	5.3 ± 1.8	17.0 ± 2.9	20.1 ± 3.7	13.8 ± 0.8	17.1 ± 2.1	17.6 ± 0.8
word_length	31.0 ± 2.2	36.5 ± 2.1	37.6 ± 0.6	33.4 ± 1.4	40.2 ± 2.2	38.4 ± 2.2	28.5 ± 1.1	39.9 ± 1.9	40.0 ± 3.2	31.5 ± 1.0	41.1 ± 2.4	36.6 ± 1.1
ICL composite (macro) ↑	13.3 ± 1.2	20.6 ± 1.3	33.4 ± 1.4	10.7 ± 0.9	17.8 ± 1.2	27.9 ± 1.3	10.4 ± 1.1	18.7 ± 1.6	27.2 ± 1.5	11.8 ± 1.0	21.6 ± 1.5	27.0 ± 1.2

Table 12: Function-probe suite of Todd et al. (2024): HITS@1 accuracy on 10-shots prompts, reported as mean±std across three seeds, for 0.13B, 0.5B, and 1B, comparing Clean run, top-2% induction heads drop (↓**Induct Hd 2%**), random heads drop (↓**Rand**) across Baseline, Induction, Anti, and Balanced curricula.

	Baseline								
	0.13B			0.5B			1B		
	Clean	↓Induct Hd 2%	↓Rand	Clean	↓Induct Hd 2%	↓Rand	Clean	↓Induct Hd 2%	↓Rand
alphabetically_first_3	4.86 ± 0.62	3.74 ± 0.66	5.69 ± 0.37	9.40 ± 0.57	8.86 ± 0.56	8.83 ± 0.58	19.71 ± 0.90	15.00 ± 0.86	19.51 ± 0.96
alphabetically_first_5	3.97 ± 0.57	3.43 ± 0.52	5.40 ± 0.94	6.71 ± 0.83	7.74 ± 0.66	6.69 ± 1.29	12.37 ± 1.41	11.03 ± 0.93	12.31 ± 1.14
alphabetically_last_3	3.37 ± 0.55	2.74 ± 0.34	4.69 ± 0.71	10.23 ± 0.88	8.40 ± 0.55	9.17 ± 0.77	20.80 ± 0.64	16.31 ± 1.23	18.80 ± 1.01
alphabetically_last_5	2.51 ± 0.75	2.09 ± 0.37	3.80 ± 0.78	6.03 ± 1.30	6.11 ± 1.36	6.06 ± 0.34	9.89 ± 0.82	9.20 ± 0.87	9.83 ± 0.76
capitalize	8.00 ± 1.03	7.02 ± 0.62	9.93 ± 0.83	20.70 ± 1.40	13.19 ± 1.17	15.09 ± 1.61	54.81 ± 2.05	36.74 ± 2.61	52.42 ± 2.48
capitalize_first_letter	10.07 ± 1.18	7.89 ± 0.98	13.30 ± 1.15	12.53 ± 1.77	11.05 ± 1.70	10.88 ± 1.36	28.56 ± 1.08	22.70 ± 0.52	24.74 ± 0.92
capitalize_last_letter	4.84 ± 1.27	3.65 ± 0.94	5.19 ± 0.70	9.65 ± 1.05	8.98 ± 0.92	9.40 ± 1.43	8.28 ± 1.21	6.84 ± 1.27	7.61 ± 1.14
choose_first_of_3	10.34 ± 2.29	6.86 ± 0.74	11.86 ± 0.90	25.46 ± 1.76	20.11 ± 1.77	23.29 ± 1.34	69.37 ± 1.77	49.20 ± 2.03	68.80 ± 0.61
choose_first_of_5	8.66 ± 1.30	5.31 ± 1.01	10.43 ± 1.15	19.66 ± 1.94	17.63 ± 2.75	18.14 ± 2.56	55.51 ± 1.26	39.20 ± 2.13	53.71 ± 0.83
choose_last_of_3	2.03 ± 0.42	1.86 ± 0.29	2.14 ± 0.40	3.17 ± 0.16	3.17 ± 1.29	2.86 ± 0.44	4.40 ± 0.98	5.11 ± 1.18	4.23 ± 0.88
choose_last_of_5	1.51 ± 0.33	1.57 ± 0.58	2.00 ± 0.53	2.86 ± 0.61	2.46 ± 0.60	2.31 ± 0.38	3.89 ± 1.14	4.06 ± 0.65	3.63 ± 0.31
choose_middle_of_3	1.69 ± 0.64	1.49 ± 0.16	1.83 ± 0.60	3.34 ± 0.55	3.31 ± 0.48	3.06 ± 0.47	4.23 ± 0.48	4.94 ± 0.52	4.37 ± 0.59
choose_middle_of_5	1.63 ± 0.30	1.63 ± 0.46	2.00 ± 0.73	2.97 ± 0.64	3.29 ± 0.48	2.69 ± 0.52	2.71 ± 0.36	3.23 ± 0.56	2.89 ± 0.34
lowercase_first_letter	5.51 ± 0.77	4.74 ± 0.99	7.72 ± 1.05	8.42 ± 0.86	7.26 ± 1.02	7.72 ± 1.11	28.53 ± 2.16	24.63 ± 1.69	26.60 ± 1.94
lowercase_last_letter	11.09 ± 0.85	7.51 ± 1.80	8.49 ± 1.63	7.72 ± 0.73	7.37 ± 0.98	7.54 ± 1.19	10.46 ± 1.09	10.32 ± 1.00	8.81 ± 1.20
next_capital_letter	4.88 ± 1.09	3.19 ± 0.98	6.42 ± 0.59	4.21 ± 0.94	3.44 ± 1.56	4.32 ± 0.20	2.42 ± 0.81	1.86 ± 0.24	2.74 ± 0.40
next_item	3.42 ± 2.17	2.78 ± 2.03	5.19 ± 1.22	8.61 ± 2.48	5.95 ± 2.26	13.16 ± 1.51	16.84 ± 2.13	17.09 ± 1.10	16.08 ± 0.57
prev_item	2.53 ± 0.78	2.03 ± 1.44	3.67 ± 1.51	7.72 ± 1.64	5.32 ± 1.15	11.39 ± 1.85	15.06 ± 2.30	15.82 ± 1.10	14.68 ± 1.13
word_length	9.89 ± 0.99	9.19 ± 1.06	8.74 ± 1.05	13.33 ± 0.94	11.96 ± 0.67	12.70 ± 1.76	12.77 ± 1.11	13.12 ± 0.68	12.07 ± 1.87
ICL Composite (macro)	5.3 ± 0.9	4.1 ± 0.8	6.2 ± 0.9	9.6 ± 1.1	8.2 ± 1.2	9.2 ± 1.1	20.0 ± 1.3	16.1 ± 1.1	19.2 ± 1.0

	Induction								
	0.13B			0.5B			1B		
	Clean	↓Induct Hd 2%	↓Rand	Clean	↓Induct Hd 2%	↓Rand	Clean	↓Induct Hd 2%	↓Rand
alphabetically_first_3	4.63 ± 0.57	4.43 ± 0.93	4.14 ± 0.53	7.34 ± 0.33	5.89 ± 0.57	7.03 ± 0.48	15.11 ± 0.89	12.94 ± 0.81	15.09 ± 0.91
alphabetically_first_5	4.23 ± 0.79	4.89 ± 0.42	4.57 ± 0.44	6.51 ± 1.03	6.46 ± 0.74	6.94 ± 0.80	10.89 ± 0.87	9.09 ± 0.65	9.63 ± 1.21
alphabetically_last_3	2.43 ± 0.54	2.31 ± 0.40	2.54 ± 0.55	7.69 ± 0.16	7.29 ± 0.77	7.83 ± 0.56	15.77 ± 0.96	12.31 ± 0.64	15.94 ± 0.97
alphabetically_last_5	1.60 ± 0.27	1.31 ± 0.48	1.89 ± 0.12	5.49 ± 0.39	5.40 ± 0.99	6.06 ± 0.61	8.51 ± 0.33	7.51 ± 1.21	8.97 ± 0.62
capitalize	3.33 ± 0.28	3.75 ± 1.09	4.56 ± 0.25	13.19 ± 1.27	12.00 ± 1.28	14.84 ± 1.24	33.37 ± 1.31	25.93 ± 0.72	31.30 ± 1.15
capitalize_first_letter	5.33 ± 1.00	5.40 ± 1.11	5.26 ± 0.62	13.40 ± 1.65	11.40 ± 1.16	14.14 ± 1.27	13.68 ± 1.16	11.58 ± 1.41	14.28 ± 1.23
capitalize_last_letter	8.63 ± 1.12	10.88 ± 0.66	6.81 ± 0.70	7.51 ± 1.75	7.09 ± 0.88	5.93 ± 0.95	8.63 ± 0.85	9.33 ± 1.17	7.30 ± 0.90
choose_first_of_3	6.14 ± 0.89	4.80 ± 0.85	6.11 ± 0.67	19.03 ± 1.72	15.14 ± 1.55	20.06 ± 2.31	52.37 ± 2.00	41.03 ± 2.98	52.89 ± 1.19
choose_first_of_5	4.86 ± 0.73	4.23 ± 0.39	5.26 ± 0.58	15.31 ± 0.91	11.74 ± 1.82	16.31 ± 1.40	42.63 ± 3.05	33.89 ± 3.08	43.63 ± 1.43
choose_last_of_3	1.43 ± 0.44	1.63 ± 0.34	1.94 ± 0.28	2.83 ± 0.26	2.54 ± 1.13	2.66 ± 0.52	5.40 ± 0.92	5.77 ± 1.38	5.63 ± 0.96
choose_last_of_5	1.74 ± 0.47	1.63 ± 0.55	2.26 ± 0.44	2.37 ± 0.41	1.94 ± 0.16	2.69 ± 0.63	4.57 ± 0.58	4.86 ± 0.61	4.03 ± 0.62
choose_middle_of_3	2.11 ± 0.80	1.86 ± 0.53	1.89 ± 0.51	2.23 ± 0.26	2.09 ± 0.41	2.37 ± 0.30	6.00 ± 1.03	5.51 ± 0.36	5.51 ± 0.64
choose_middle_of_5	1.60 ± 0.23	1.63 ± 0.49	1.60 ± 0.53	2.09 ± 0.28	1.66 ± 0.46	1.86 ± 0.48	3.09 ± 0.62	3.66 ± 0.52	3.03 ± 0.63
lowercase_first_letter	4.14 ± 0.92	2.63 ± 0.30	6.00 ± 1.31	6.07 ± 1.23	5.61 ± 0.72	7.26 ± 0.75	20.11 ± 1.56	17.05 ± 1.46	18.21 ± 1.22
lowercase_last_letter	3.61 ± 0.67	2.84 ± 0.34	3.65 ± 1.16	8.04 ± 0.73	7.86 ± 1.48	8.18 ± 1.72	9.61 ± 0.96	9.26 ± 0.44	7.68 ± 1.43
next_capital_letter	3.86 ± 0.33	4.28 ± 1.08	3.82 ± 0.78	4.18 ± 0.96	4.04 ± 0.83	3.44 ± 0.64	3.58 ± 0.72	3.47 ± 0.68	3.09 ± 0.36
next_item	2.91 ± 1.93	2.66 ± 1.58	4.30 ± 2.07	5.70 ± 1.34	6.46 ± 1.44	7.72 ± 1.76	11.77 ± 1.23	11.14 ± 2.03	12.91 ± 2.13
prev_item	2.03 ± 0.83	2.78 ± 1.31	3.04 ± 1.04	5.95 ± 0.72	6.71 ± 0.96	6.20 ± 1.70	10.25 ± 1.04	9.62 ± 2.16	9.49 ± 1.34
word_length	13.40 ± 0.83	10.21 ± 0.98	13.86 ± 1.67	14.00 ± 0.97	11.79 ± 0.57	12.49 ± 1.31	13.33 ± 0.84	12.18 ± 1.10	13.26 ± 1.19
ICL Composite (macro)	4.1 ± 0.7	3.9 ± 0.7	4.4 ± 0.8	7.8 ± 0.9	7.0 ± 0.9	8.1 ± 1.0	15.2 ± 1.1	13.0 ± 1.2	14.8 ± 1.1

	Anti-Induction								
	0.13B			0.5B			1B		
	Clean	↓Induct Hd 2%	↓Rand	Clean	↓Induct Hd 2%	↓Rand	Clean	↓Induct Hd 2%	↓Rand
alphabetically_first_3	3.34 ± 0.55	2.83 ± 0.50	3.57 ± 0.45	8.46 ± 0.88	7.40 ± 0.26	8.00 ± 0.51	14.43 ± 1.47	11.34 ± 1.13	14.49 ± 1.33
alphabetically_first_5	2.83 ± 0.68	2.57 ± 0.34	2.71 ± 0.30	7.37 ± 0.63	7.69 ± 0.23	7.80 ± 1.03	8.43 ± 1.15	7.97 ± 0.76	9.11 ± 0.80
alphabetically_last_3	1.94 ± 0.60	2.20 ± 0.30	2.60 ± 0.40	7.97 ± 0.87	7.71 ± 0.61	7.63 ± 0.58	13.26 ± 0.77	10.40 ± 0.75	13.80 ± 0.46
alphabetically_last_5	1.77 ± 0.36	1.49 ± 0.58	2.09 ± 0.59	6.06 ± 0.79	5.89 ± 0.91	6.94 ± 0.59	7.80 ± 0.48	7.14 ± 0.83	8.29 ± 0.42
capitalize	3.72 ± 0.15	5.33 ± 1.26	4.67 ± 0.75	13.47 ± 1.33	11.16 ± 1.34	13.30 ± 1.62	39.23 ± 2.71	34.18 ± 1.46	37.40 ± 0.83
capitalize_first_letter	5.19 ± 0.32	6.11 ± 2.06	5.58 ± 0.45	11.16 ± 1.21	10.56 ± 1.75	10.67 ± 1.33	17.44 ± 0.84	17.65 ± 2.57	20.98 ± 1.51
capitalize_last_letter	9.09 ± 1.39	6.74 ± 1.56	7.93 ± 1.13	9.30 ± 1.16	8.39 ± 0.89	8.04 ± 1.22	7.26 ± 1.49	6.67 ± 0.76	6.32 ± 1.40
choose_first_of_3	4.11 ± 0.72	3.60 ± 0.21	3.83 ± 0.36	19.06 ± 1.75	16.69 ± 1.56	19.60 ± 1.64	46.03 ± 2.04	34.43 ± 1.29	46.31 ± 1.30
choose_first_of_5	3.63 ± 0.67	2.69 ± 0.40	3.17 ± 0.38	16.20 ± 1.49	14.43 ± 1.66	17.49 ± 1.29	32.69 ± 1.64	23.97 ± 0.53	33.71 ± 1.21
choose_last_of_3	1.40 ± 0.51	0.94 ± 0.19	0.94 ± 0.13	2.97 ± 0.52	3.34 ± 0.50	3.46 ± 1.11	5.00 ± 0.51	5.11 ± 0.86	5.03 ± 1.18
choose_last_of_5	1.09 ± 0.37	0.97 ± 0.33	1.31 ± 0.31	2.86 ± 0.52	2.66 ± 0.26	2.51 ± 0.47	5.63 ± 0.47	5.06 ± 0.52	4.86 ± 0.92
choose_middle_of_3	1.34 ± 0.52	1.31 ± 0.70	1.43 ± 0.23	3.09 ± 0.24	2.63 ± 0.52	2.94 ± 0.52	4.97 ± 0.27	4.97 ± 0.31	4.83 ± 0.93
choose_middle_of_5	1.66 ± 0.36	1.71 ± 0.44	1.57 ± 0.39	2.86 ± 0.69	2.86 ± 0.30	1.94 ± 0.52	3.89 ± 0.73	3.71 ± 0.27	3.34 ± 0.89
lowercase_first_letter	4.67 ± 0.74	3.61 ± 0.97	4.98 ± 1.01	6.53 ± 0.59	6.56 ± 1.17	7.58 ± 0.60	20.56 ± 1.11	18.74 ± 1.52	18.98 ± 1.86
lowercase_last_letter	7.37 ± 1.15	5.47 ± 0.64	8.18 ± 1.45	8.88 ± 0.97	9.26 ± 0.73	8.04 ± 1.58	13.26 ± 0.47	12.46 ± 1.75	12.67 ± 1.57
next_capital_letter	4.67 ± 0.79	5.05 ± 1.24	5.09 ± 0.92	4.14 ± 0.71	3.65 ± 0.57	4.04 ± 0.55	3.05 ± 0.91	3.19 ± 0.60	2.98 ± 0.79
next_item	1.27 ± 0.90	2.15 ± 0.72	2.41 ± 1.37	7.85 ± 1.06	6.71 ± 2.71	6.71 ± 0.72	11.77 ± 2.48	12.41 ± 2.31	13.04 ± 1.15
prev_item	1.39 ± 0.53	2.28 ± 1.65	1.77 ± 0.28	6.58 ± 2.52	5.70 ± 1.85	7.09 ± 0.83	11.39 ± 2.45	12.03 ± 1.00	10.89 ± 1.44
word_length	12.00 ± 1.29	11.05 ± 1.20	11.40 ± 1.59	14.32 ± 0.58	13.33 ± 0.75	14.18 ± 1.68	13.58 ± 1.60	12.49 ± 1.83	13.37 ± 1.69
ICL Composite (macro)	3.8 ± 0.7	3.6 ± 0.8	4.0 ± 0.7	8.4 ± 1.0	7.7 ± 1.0	8.3 ± 1.0	14.7 ± 1.2	12.8 ± 1.1	14.8 ± 1.1

	Balanced								
	0.13B			0.5B			1B		
	Clean	↓Induct Hd 2%	↓Rand	Clean	↓Induct Hd 2%	↓Rand	Clean	↓Induct Hd 2%	↓Rand
alphabetically_first_3	4.83 ± 0.62	3.17 ± 0.37	4.71 ± 0.80	11.54 ± 0.60	9.54 ± 0.47	11.26 ± 1.04	15.31 ± 0.96	13.66 ± 0.58	14.83 ± 0.68
alphabetically_first_5	3.94 ± 0.97	3.14 ± 0.83	4.26 ± 0.93	8.23 ± 0.78	6.80 ± 0.67	8.11 ± 1.16	10.20 ± 0.70	9.11 ± 0.69	10.26 ± 0.72
alphabetically_last_3	3.94 ± 0.47	2.00 ± 0.53	4.74 ± 0.43	10.89 ± 0.50	9.71 ± 0.66	11.49 ± 0.16	15.34 ± 1.35	13.91 ± 0.46	15.20 ± 0.78
alphabetically_last_5	2.51 ± 0.77	1.34 ± 0.22	2.14 ± 0.35	6.71 ± 0.55	6.54 ± 0.64	7.09 ± 0.41	9.31 ± 0.43	9.37 ± 0.63	9.63 ± 0.50
capitalize	6.00 ± 1.63	5.65 ± 1.06	7.09 ± 1.12	14.67 ± 1.30	14.49 ± 1.15	12.77 ± 1.99	33.65 ± 2.14	27.93 ± 1.35	31.82 ± 1.33
capitalize_first_letter	8.88 ± 0.66	7.75 ± 1.39	9.44 ± 0.96	10.00 ± 1.07	11.65 ± 1.76	10.98 ± 2.45	20.39 ± 1.17	18.84 ± 1.32	19.26 ± 1.54
capitalize_last_letter	5.51 ± 0.67	5.65 ± 0.57	4.04 ± 0.92	5.75 ± 1.38	7.37 ± 0.67	5.33 ± 1.26	6.67 ± 0.66	5.68 ± 1.68	6.11 ± 0.65
choose_first_of_3	11.29 ± 0.71	4.37 ± 0.46	11.71 ± 0.69	35.20 ± 1.70	23.49 ± 1.25	35.51 ± 2.16	54.09 ± 1.70	46.29 ± 1.12	50.03 ± 1.59
choose_first_of_5	7.89 ± 1.01	3.43 ± 0.34	7.43 ± 0.77	28.20 ± 2.41	19.31 ± 0.53	27.74 ± 2.46	42.14 ± 1.37	34.14 ± 1.15	39.91 ± 0.82
choose_last_of_3	1.69 ± 0.34	1.20 ± 0.16	1.37 ± 0.44	3.00 ± 0.53	4.00 ± 0.94	3.34 ± 0.70	5.20 ± 0.34	5.86 ± 0.91	5.69 ± 0.69
choose_last_of_5	1.46 ± 0.33	1.14 ± 0.30	1.40 ± 0.42	2.63 ± 0.36	3.09 ± 0.47	2.89 ± 0.62	5.06 ± 0.36	4.97 ± 0.42	5.80 ± 0.44
choose_middle_of_3	1.71 ± 0.66	1.20 ± 0.30	1.46 ± 0.23	3.40 ± 0.69	3.66 ± 0.58	3.11 ± 1.00	4.94 ± 0.70	5.20 ± 0.85	5.34 ± 0.63
choose_middle_of_5	1.74 ± 0.44	1.40 ± 0.47	1.69 ± 0.29	2.34 ± 0.63	3.51 ± 0.22	2.71 ± 1.04	4.66 ± 0.63	4.54 ± 0.86	4.37 ± 0.49
lowercase_first_letter	2.25 ± 0.57	4.14 ± 0.90	2.39 ± 0.69	8.84 ± 0.73	5.75 ± 0.44	9.44 ± 1.81	13.30 ± 0.84	13.61 ± 1.09	13.40 ± 1.56
lowercase_last_letter	7.82 ± 1.10	9.79 ± 1.18	7.19 ± 0.71	10.88 ± 1.53	8.84 ± 1.68	8.67 ± 1.72	8.91 ± 1.18	9.09 ± 2.06	6.56 ± 1.77
next_capital_letter	4.81 ± 0.91	3.96 ± 0.69	4.88 ± 0.88	3.47 ± 0.89	3.33 ± 0.62	4.07 ± 0.81	4.18 ± 1.15	2.56 ± 0.56	3.37 ± 0.74
next_item	6.33 ± 0.78	5.44 ± 1.82	7.85 ± 1.46	8.99 ± 1.64	8.73 ± 1.51	10.38 ± 2.85	9.37 ± 1.70	10.89 ± 1.87	9.87 ± 0.96
prev_item	5.70 ± 1.27	5.19 ± 1.13	7.97 ± 1.65	8.35 ± 1.22	9.49 ± 1.73	8.61 ± 2.39	7.72 ± 2.21	10.51 ± 0.57	7.97 ± 0.96
word_length	10.81 ± 1.09	10.14 ± 1.33	7.89 ± 0.76	14.74 ± 1.81	12.95 ± 1.16	13.51 ± 1.22	12.60 ± 0.72	12.42 ± 1.49	12.91 ± 1.60
ICL Composite (macro)	5.2 ± 0.8	4.2 ± 0.7	5.2 ± 0.8	10.4 ± 1.1	9.1 ± 0.9	10.4 ± 1.4	14.9 ± 1.1	13.6 ± 1.0	14.3 ± 1.0